GAIA : IMPROVING THE GALAXY MODELLING

A.C. Robin, Institut UTINAM, Besançon
Coll: Céline Reylé, Nadège Lagarde, Jean-Baptiste Salomon (Besançon)
Olivier Bienaymé (Strasbourg)
Roger Mor, Francesca Figueras (Barcelona)
José Fernandez-Trincado (Copiaco, Chile)

Plan

- Introduction
- New evolutionary tracks, abundances and astero-seismology
- New BGM-Fast: fast fitting of model parameters
- Clues for SFH and IMF in the thin disc from Gaia DR2
- Perspectives

Introduction

- How can we learn from a so huge survey ?
- Gaia: towards new methods : multivariate data analysis
- Gaia complemented with spectroscopy/ asteroseismology (RAVE, APOGEE, Galah, Kepler…)
- Sophisticated statistical methods needed

Introduction (2)

- Gaia is a challenge for modelling: reality much more complex than a model
- Backward / forward : complementary approaches !
- Modelling helps understand and interpret reality, even too simple
- Looking forward to improve the modelling

Besancon Galaxy Model

- Besancon Galaxy Model (BGM) elaboration and fitting
  - Use photometry, astrometry, spectroscopy
  - with bayesian exploration tools : Application to bar / thin disc fitting (Robin et al, 2012)
  - with ABC-MCMC : Applications to thick disc, halo : Constraints on density laws, structures, age and metallicity distributions (Robin et al, 2014)

Improved BGM

- New stellar evolutionary tracks (STAREVOL), provides detailed abundances (thermohaline mixing, rotation to come) (Lagarde et al, 2017, 2018)
- Improved dynamical self-consistency (Bienaymé 2015, Bienaymé et al, 2018, Bienaymé 2019)
- New 3D extinction map (Stilism, Lallement et al, 2019) based on Gaia DR2
- New fitting methods

New stellar models

- STAREVOL evolutionary tracks : with thermohaline mixing. Lagarde et al, 2017, 2018
- Simulations including abundances (and their evolution along the tracks), and astero-seismic values

BESANÇON GALAXY MODEL + STAREVOL

Robin et al (2003)
Lagarde et al (2017)

What's new ?

Include stellar evolution models computed with STAREVOL

- $M=[0.6\text{-}6.0 M_\odot]$
- [Fe/H] = {-2.15 ; -1.2 ;-0.54 ; -0.23 ; 0 ; +0.51}
- From PMS to AGB
- [α/Fe] = {0 ; 0.15 ; 0.3}

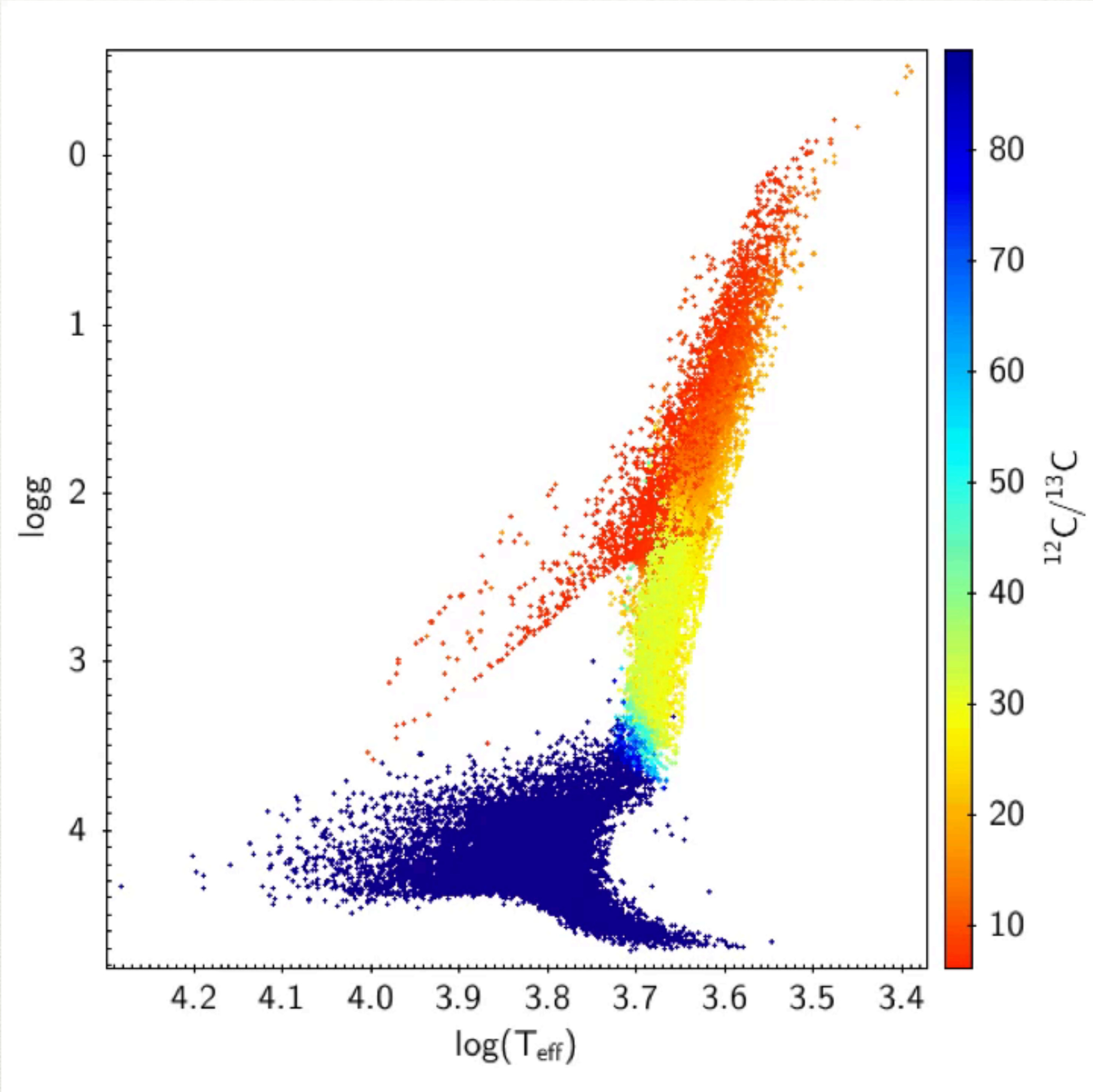

BESANÇON GALAXY MODEL + STAREVOL

Robin et al (2003)
Lagarde et al (2017)

What's new ?

Include stellar evolution models computed with STAREVOL

- M=[0.6-6.0M$_\odot$]
- [Fe/H] = {-2.15 ; -1.2 ;-0.54 ; -0.23 ; 0 ; +0.51}
- From PMS to AGB
- [α/Fe] = {0 ; 0.15 ; 0.3}

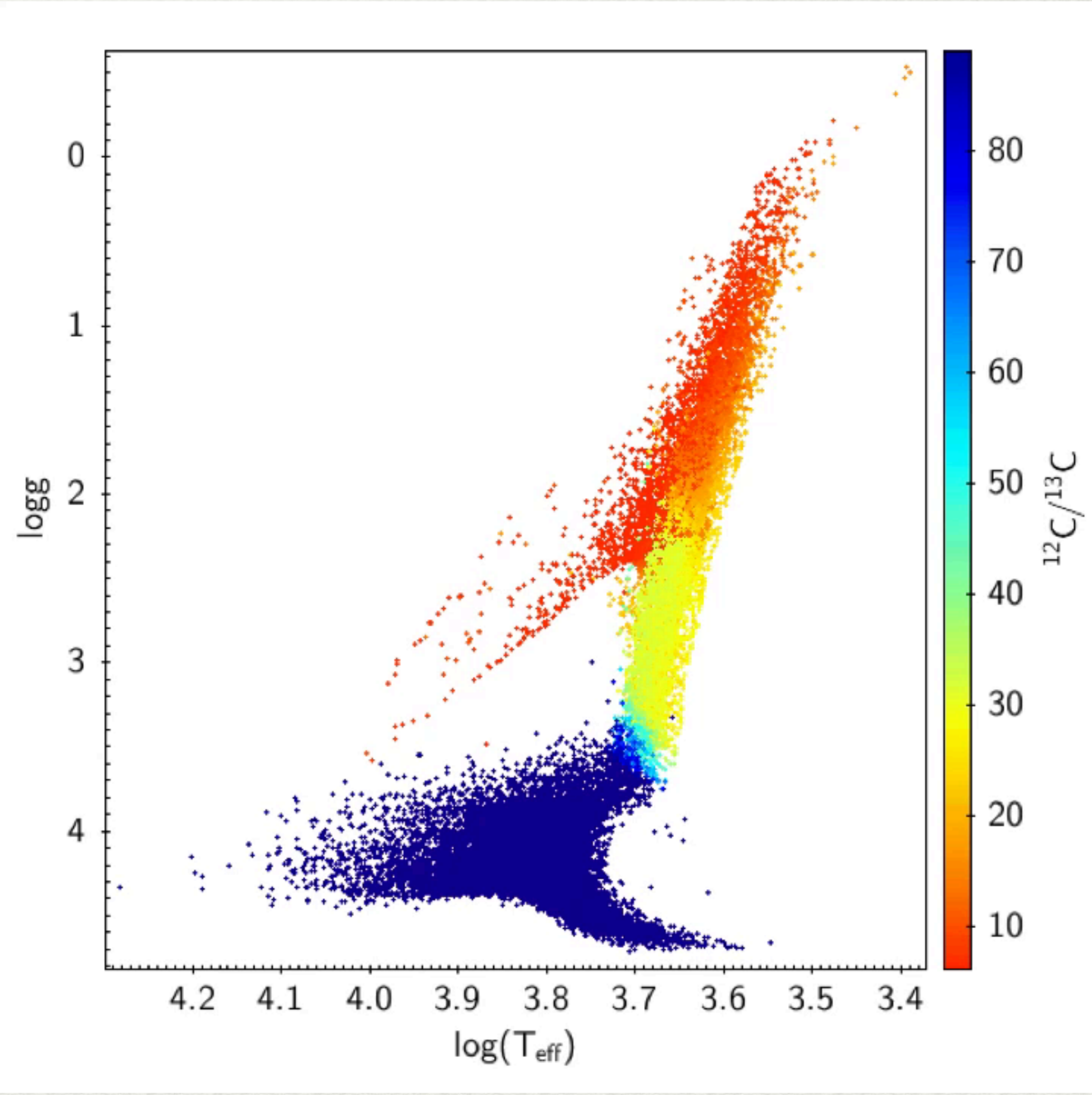

BESANÇON GALAXY MODEL + STAREVOL

Robin et al (2003)
Lagarde et al (2017)

What's new ?

Include stellar evolution models computed with STAREVOL

- M=[0.6-6.0M$_\odot$]
- [Fe/H] = {-2.15 ; -1.2 ;-0.54 ; -0.23 ; 0 ; +0.51}
- From PMS to AGB
- [α/Fe] = {0 ; 0.15 ; 0.3}

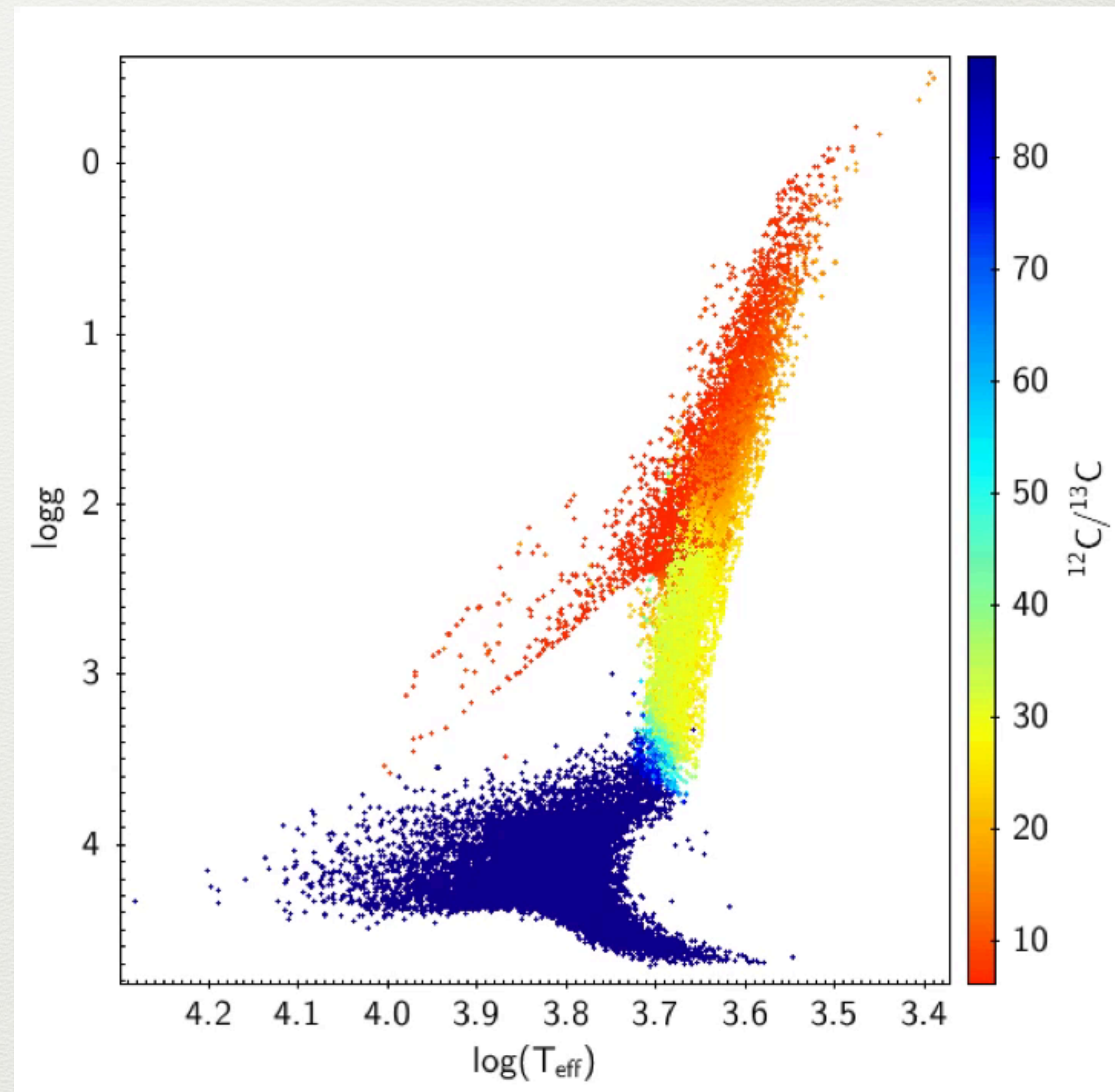

Seismic prop.

BESANÇON GALAXY MODEL + STAREVOL

Robin et al (2003)
Lagarde et al (2017)

What's new ?

Include stellar evolution models computed with STAREVOL

- $M=[0.6\text{-}6.0 M_\odot]$
- [Fe/H] = {-2.15 ; -1.2 ;-0.54 ; -0.23 ; 0 ; +0.51}
- From PMS to AGB
- [α/Fe] = {0 ; 0.15 ; 0.3}

Seismic prop.

Chemical prop.

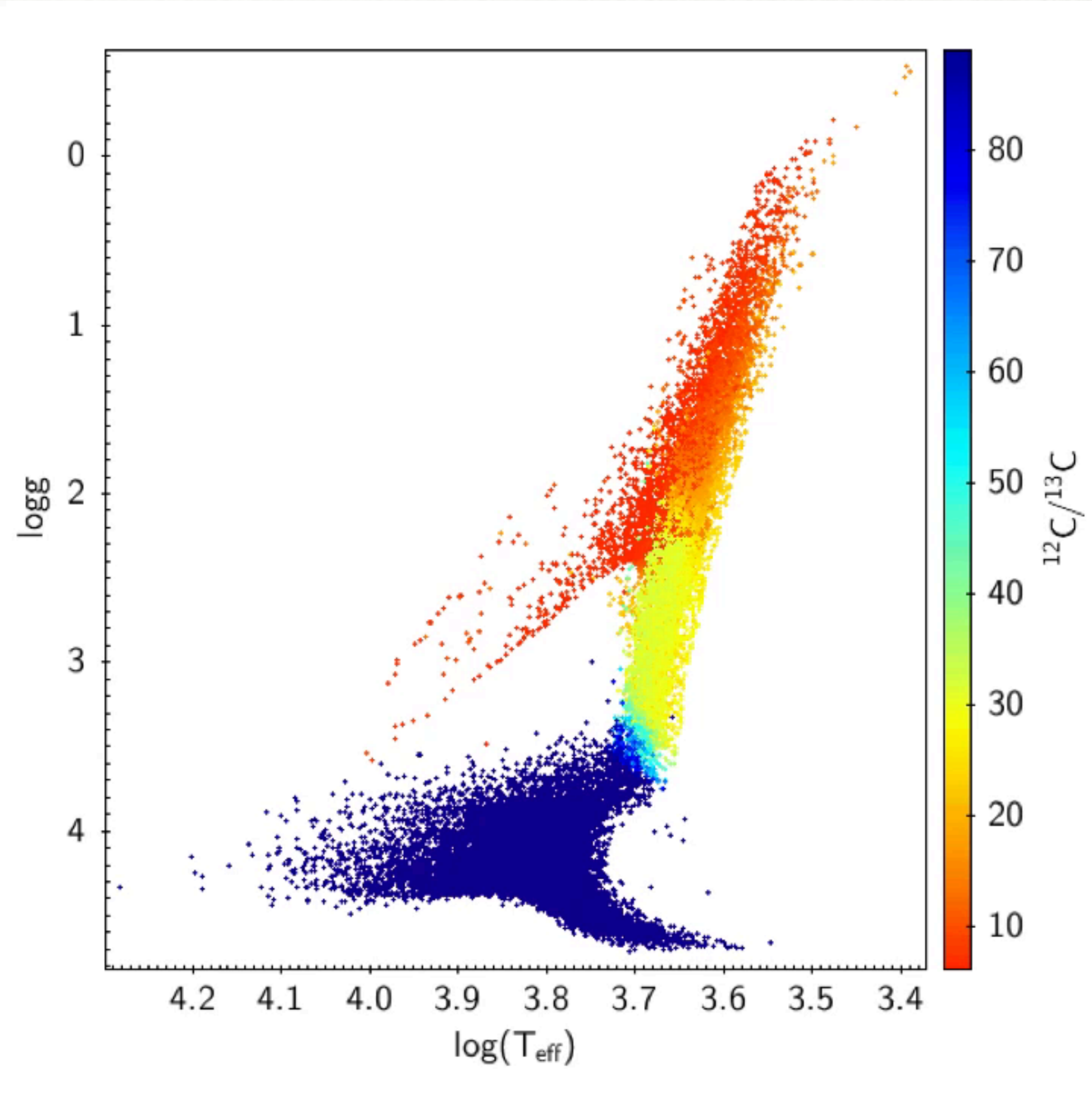

BESANÇON GALAXY MODEL + STAREVOL

Robin et al (2003)
Lagarde et al (2017)

What's new ?

Include stellar evolution models computed with STAREVOL

- M=[0.6-6.0M$_\odot$]
- [Fe/H] = {-2.15 ; -1.2 ;-0.54 ; -0.23 ; 0 ; +0.51}
- From PMS to AGB
- [α/Fe] = {0 ; 0.15 ; 0.3}

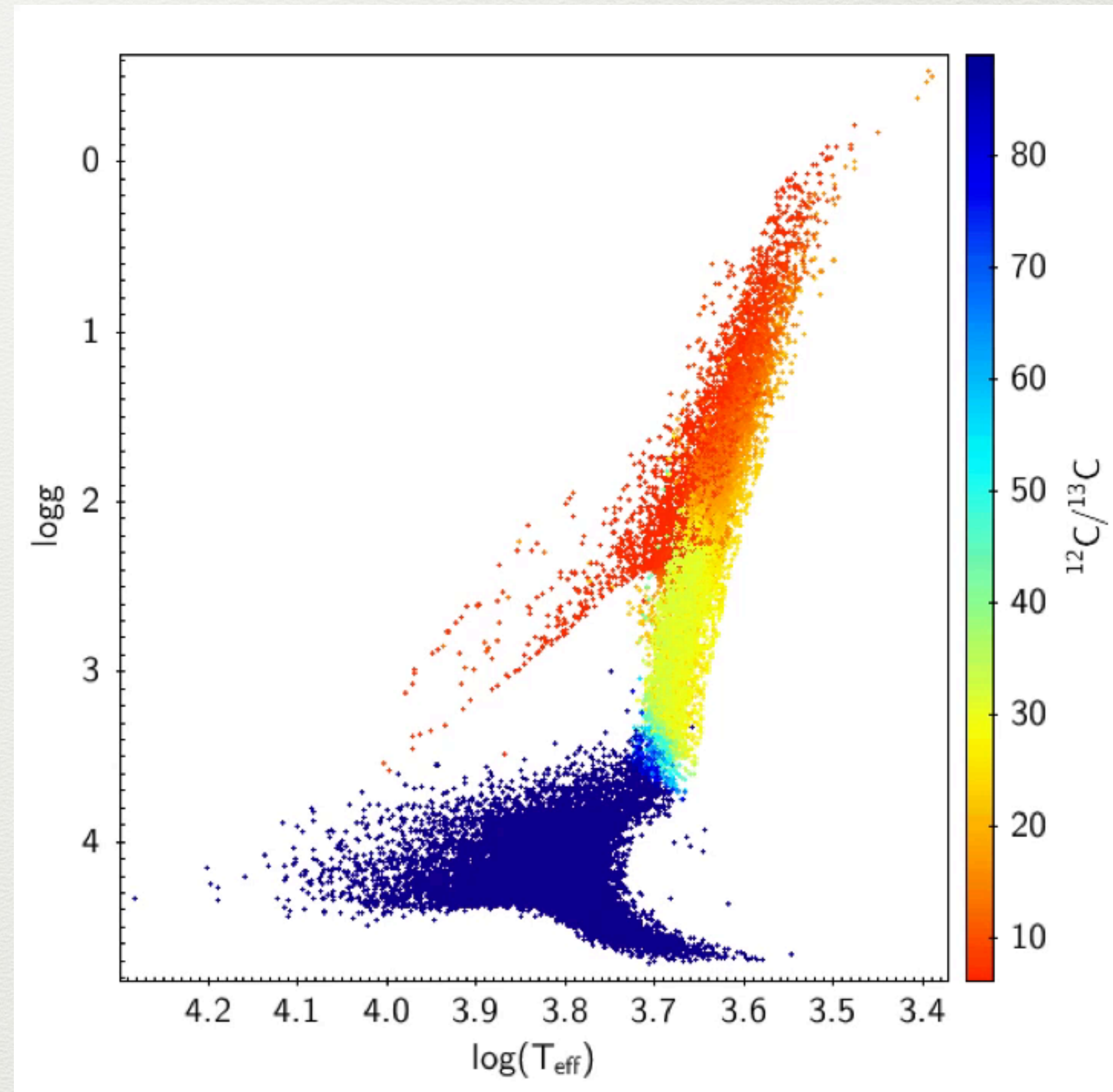

Seismic prop.

Chemical prop.

Transport processes

Charbonnel & Zahn 2007a, Charbonnel & Lagarde 2010

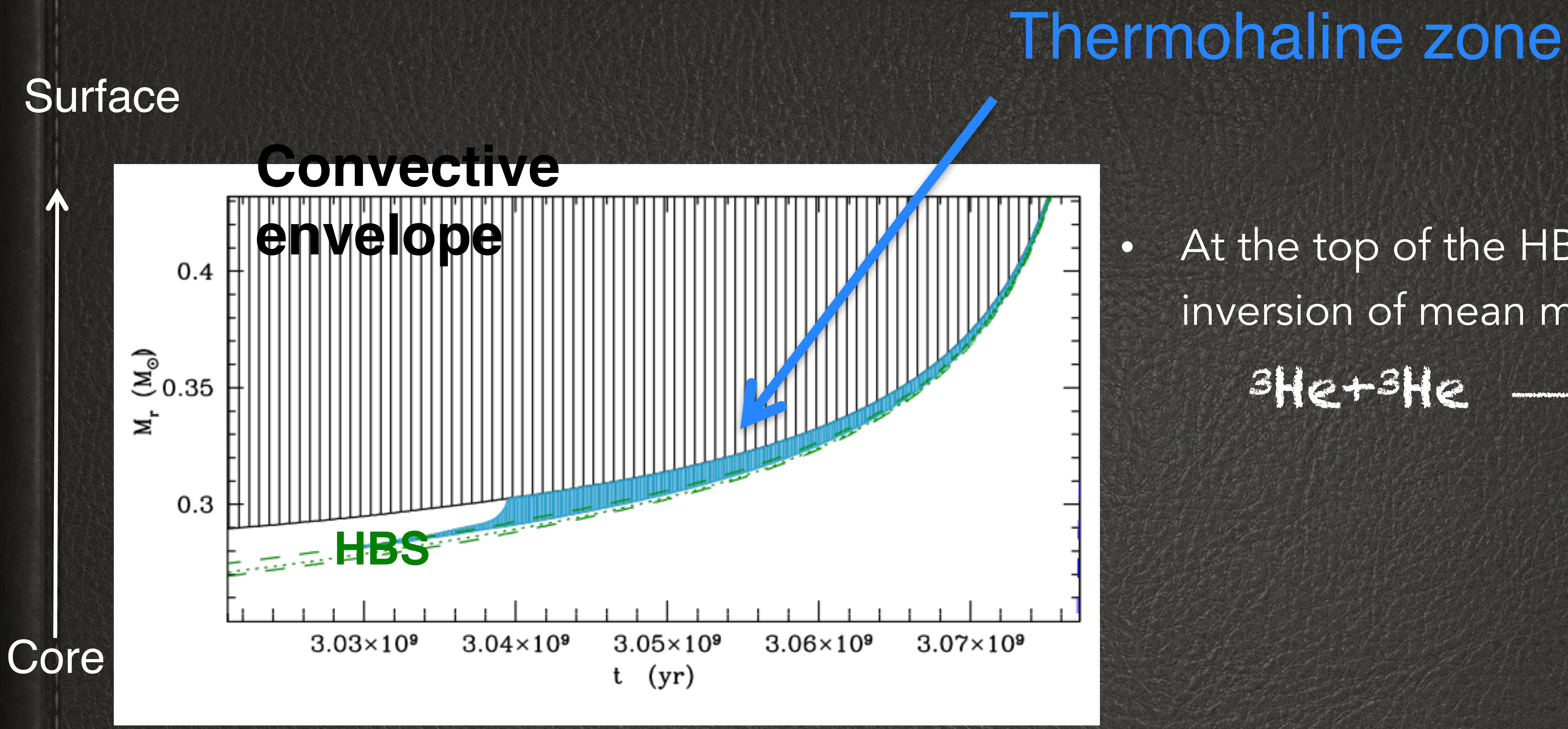

- At the top of the HBS by an inversion of mean molecular weight

$$^{3}He + ^{3}He \longrightarrow ^{4}He + 2p$$

Charbonnel & Zahn 2007a, Charbonnel & Lagarde 2010

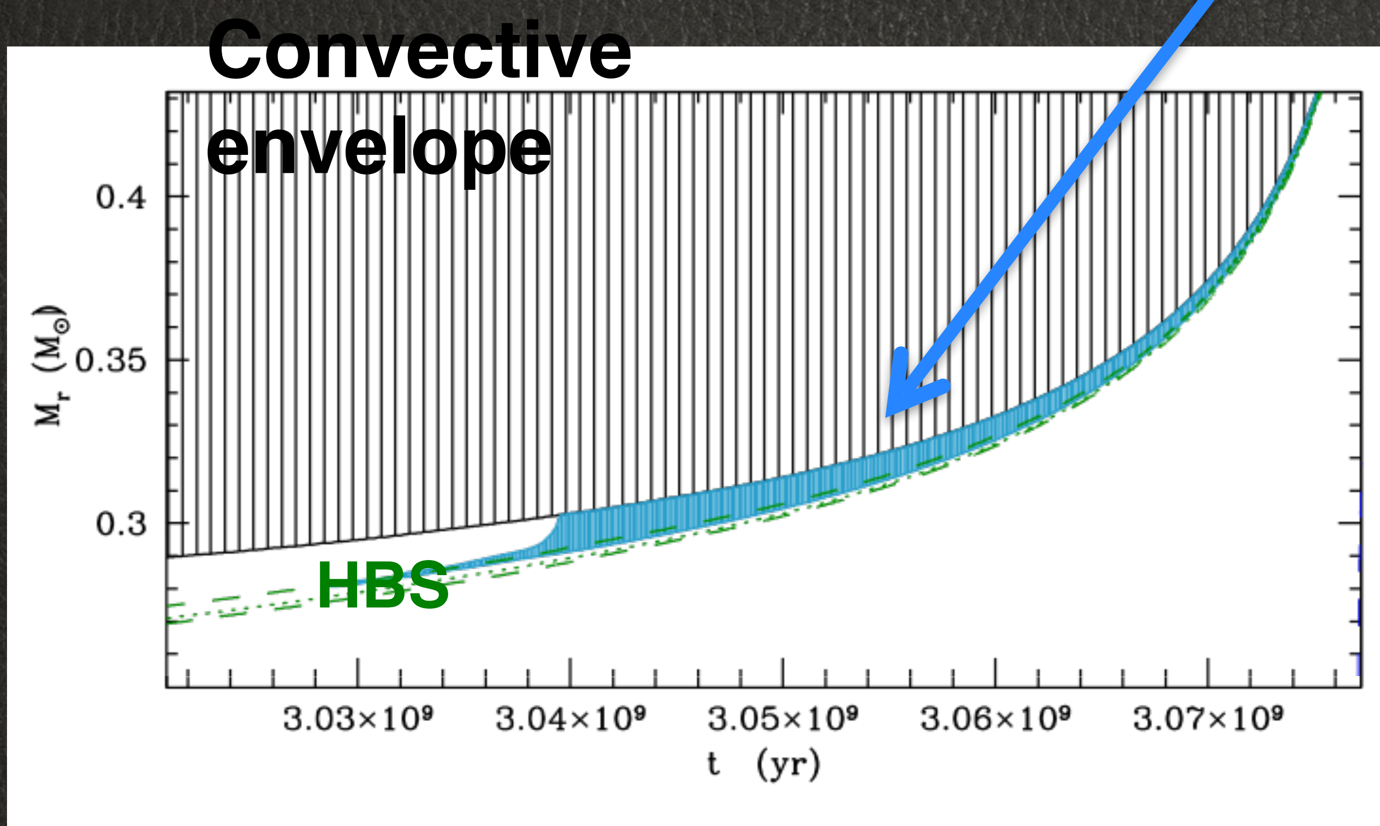

- At the top of the HBS by an inversion of mean molecular weight

  $^3He + {}^3He \longrightarrow {}^4He + 2p$

- After the star has reached the luminosity bump on the RGB

Charbonnel & Zahn 2007a, Charbonnel & Lagarde 2010

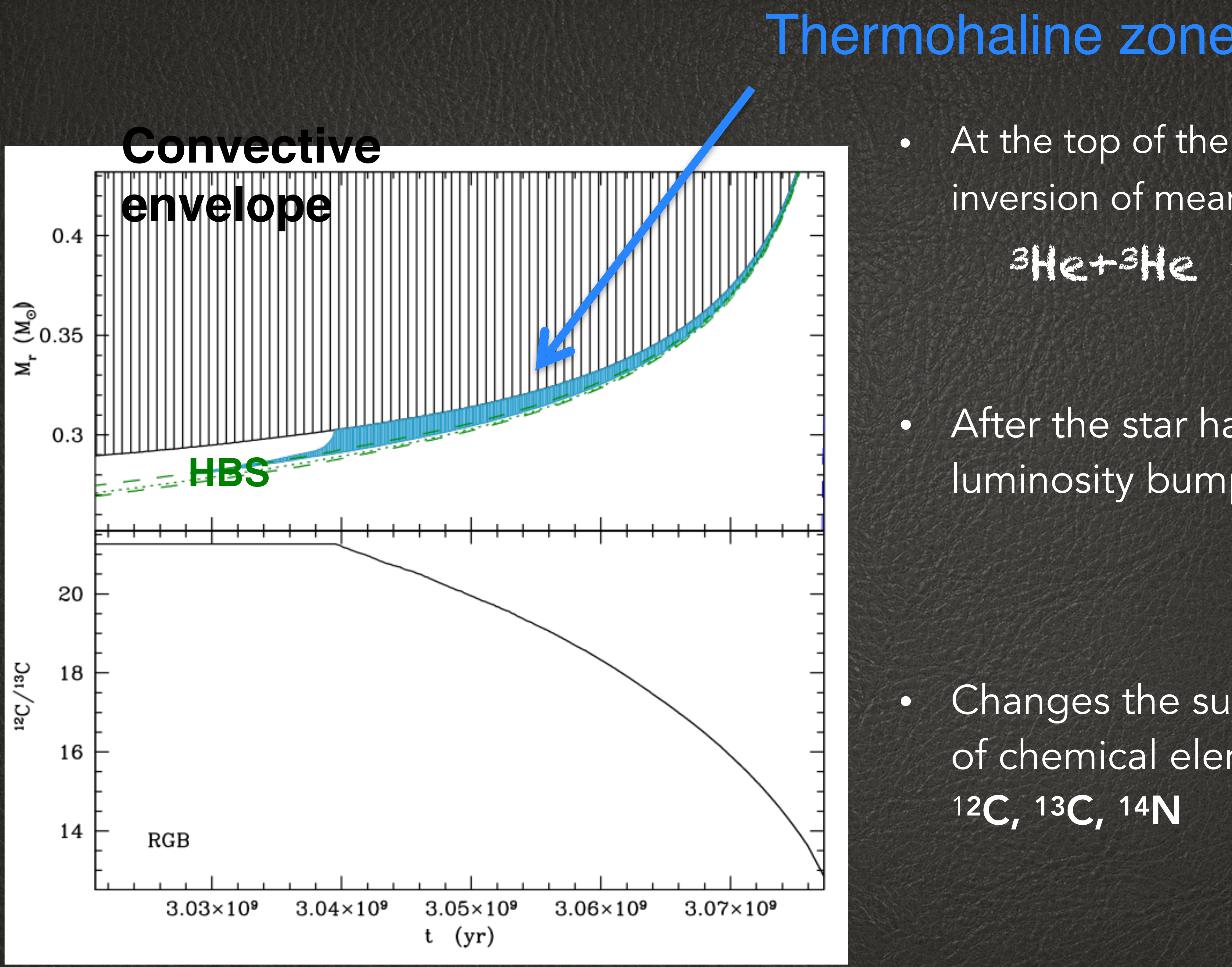

- At the top of the HBS by an inversion of mean molecular weight

  $^3He + ^3He \longrightarrow ^4He + 2p$

- After the star has reached the luminosity bump on the RGB

- Changes the surface abundances of chemical elements as Li, ^{3}**He**, ^{12}**C**, ^{13}**C**, ^{14}**N**

Besançon population synthesis model
Lagarde et al (2017)

→

For all stars in the Milky Way (thin, thick, halo and bulge):

- Seismic prop.
  $\Delta\nu$, ν_{max}, $\Delta\Pi$
- Chemical prop.
  C, N, O, …
- Effects of mixing

Effect of thermo-Haline mixing at different stages

On [C/N]

Grey: no mixing
Colored: thermo-haline mixing
Colored by metallicity

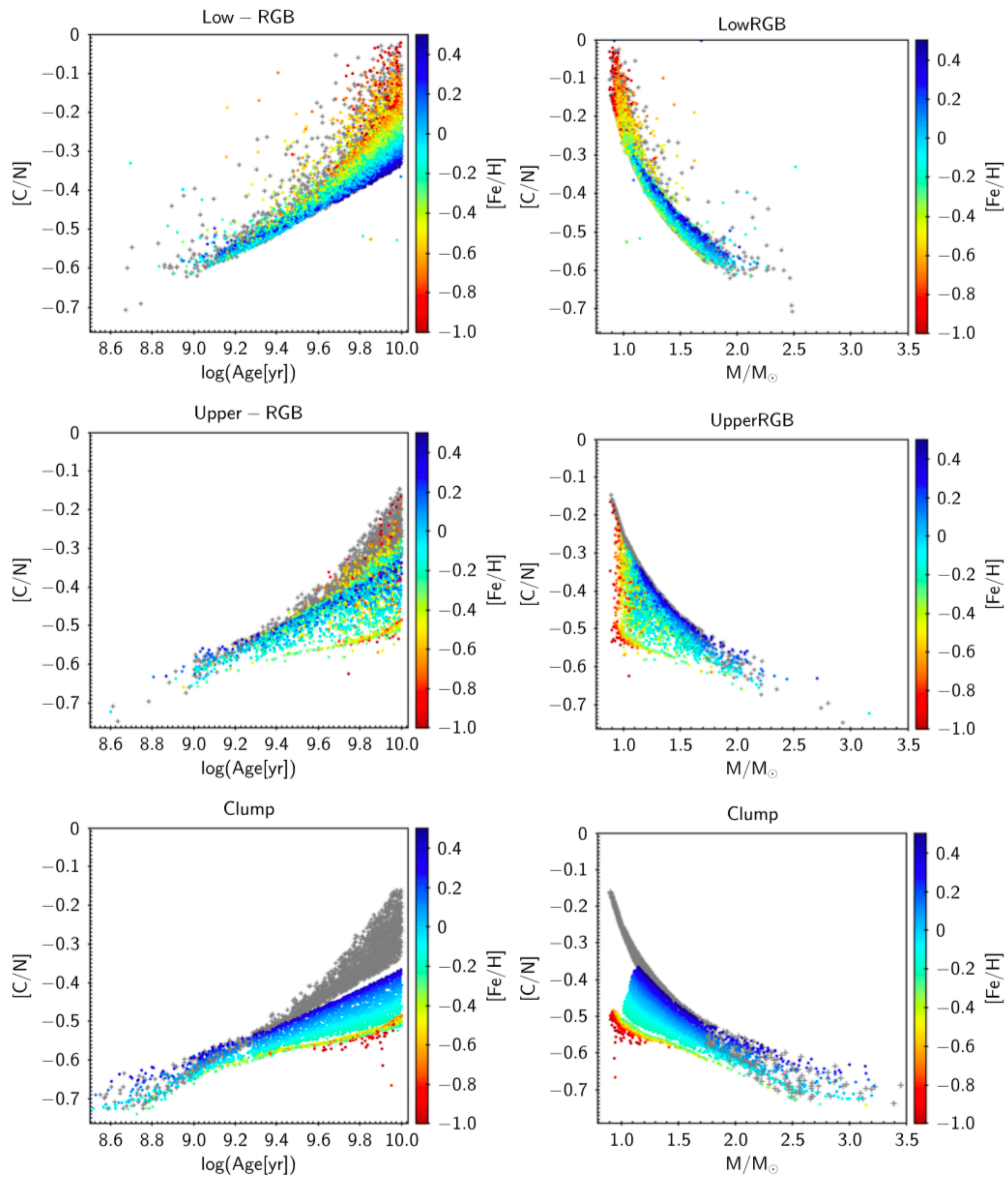

Fig. 5. Surface abundance of [C/N] as a function of stellar ages (*left panels*) and stellar masses (*right panels*), colour-coded by metallicity, for a synthetic thin disc computed with the BGM. Stars have been selected to be in the clump according to their $\Delta\Pi_{\ell=1}$, as well as before and after the RGB-bump according to their log(g) values. Simulations including or not the effect of thermohaline instability are shown as colour-dots and grey crosses respectively.

[C/N] vs Age

Lagarde et al 2017

Standard models

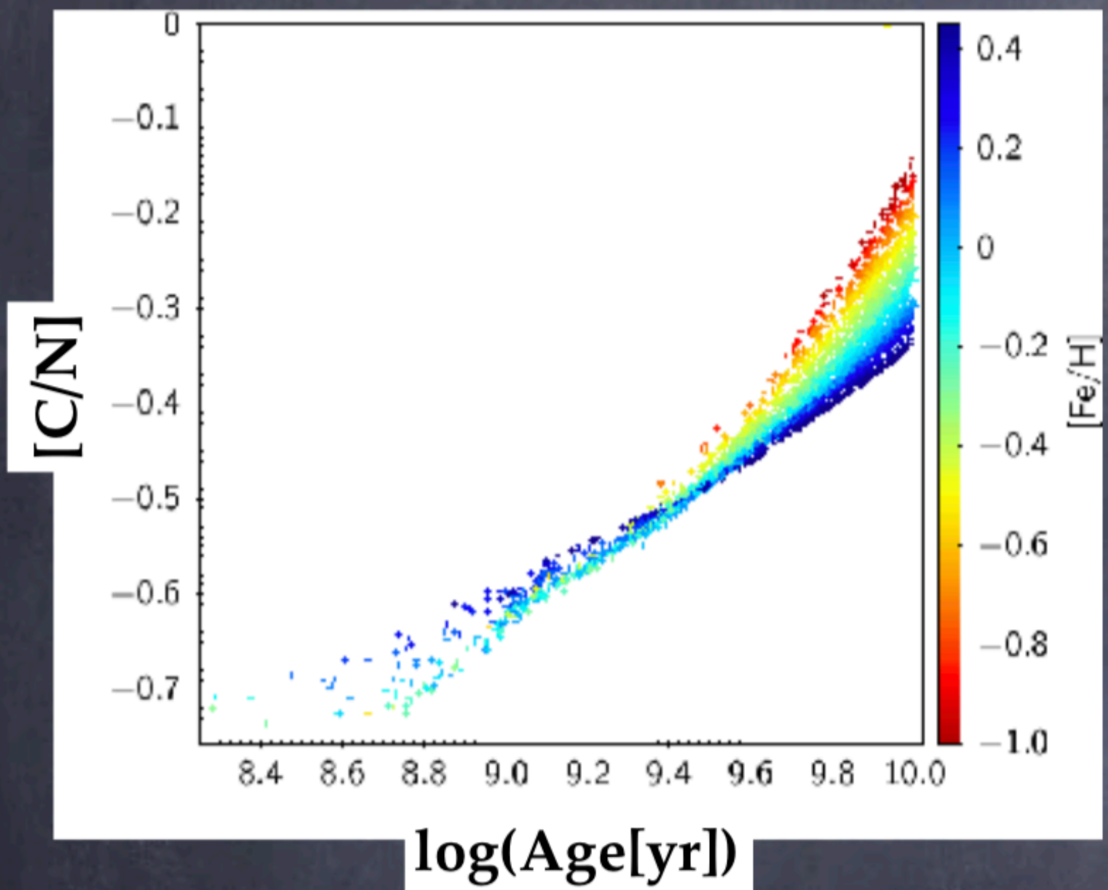

Thermohaline models

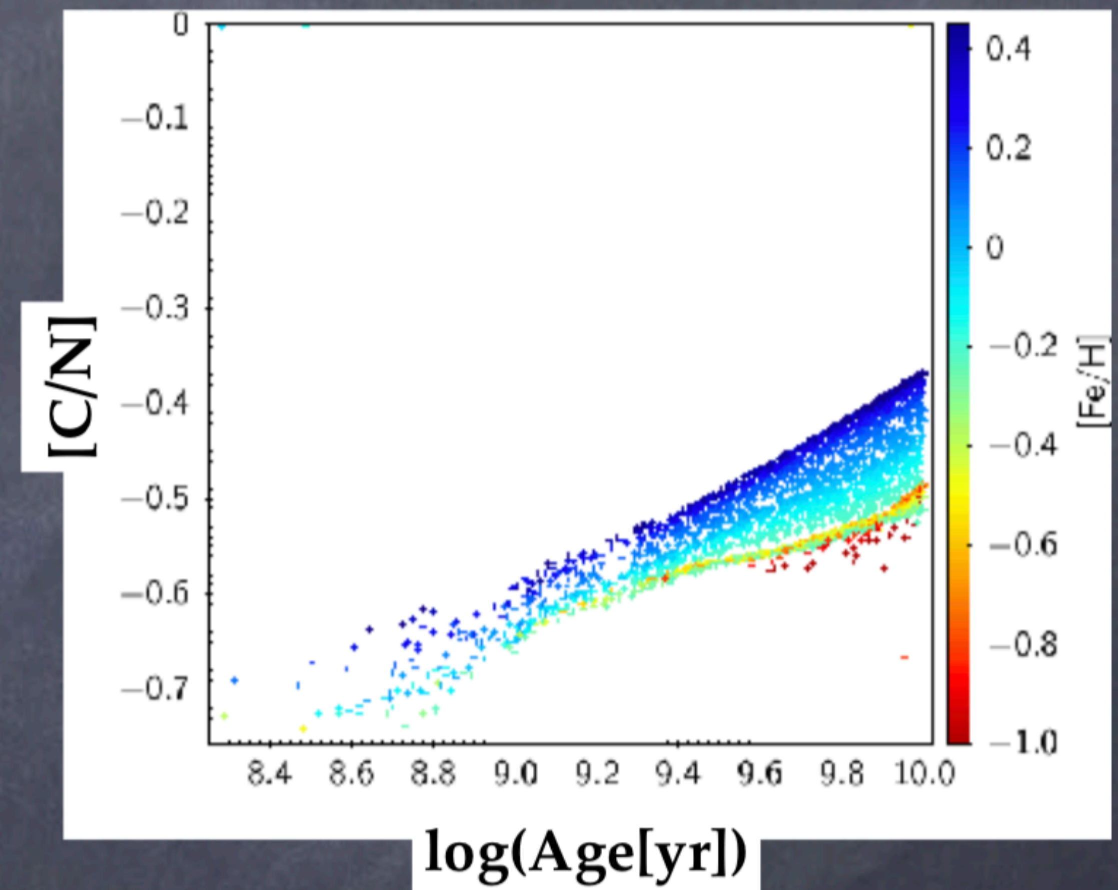

Clump stars

[C/N] vs Age

Lagarde et al 2017

Standard models

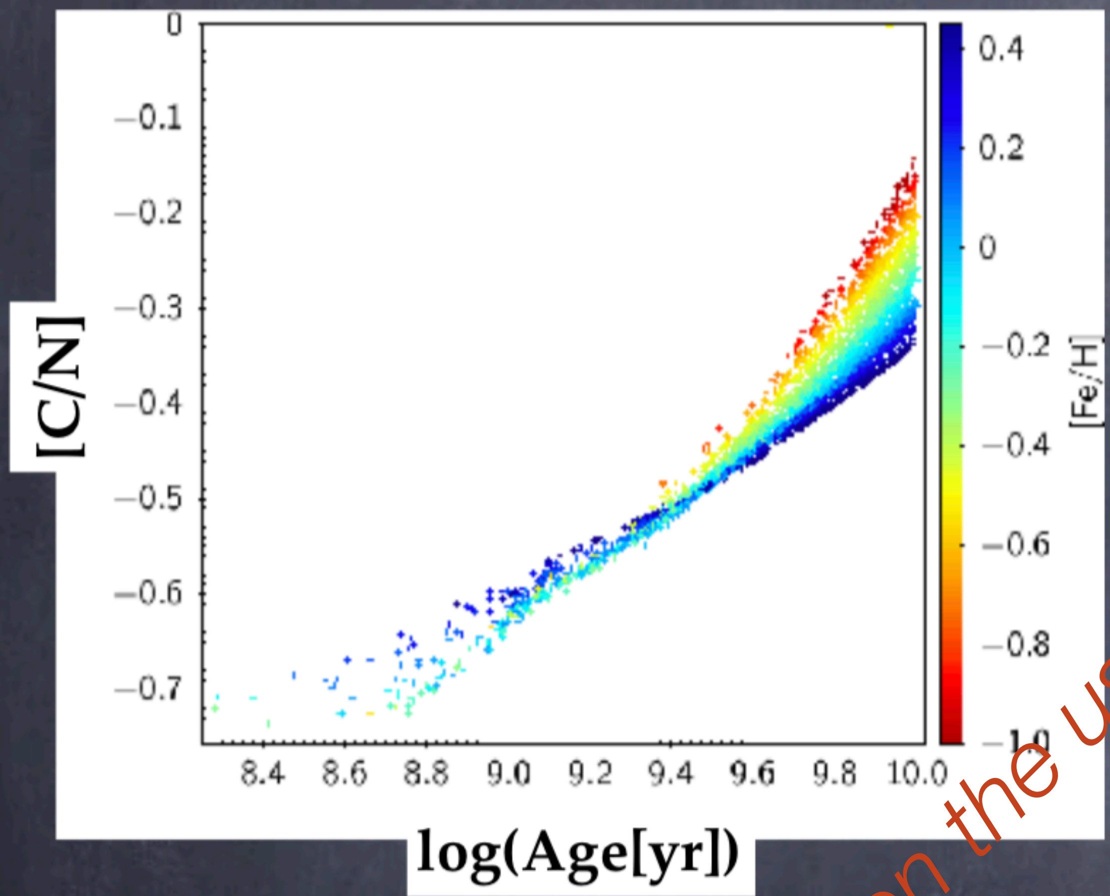

Thermohaline models

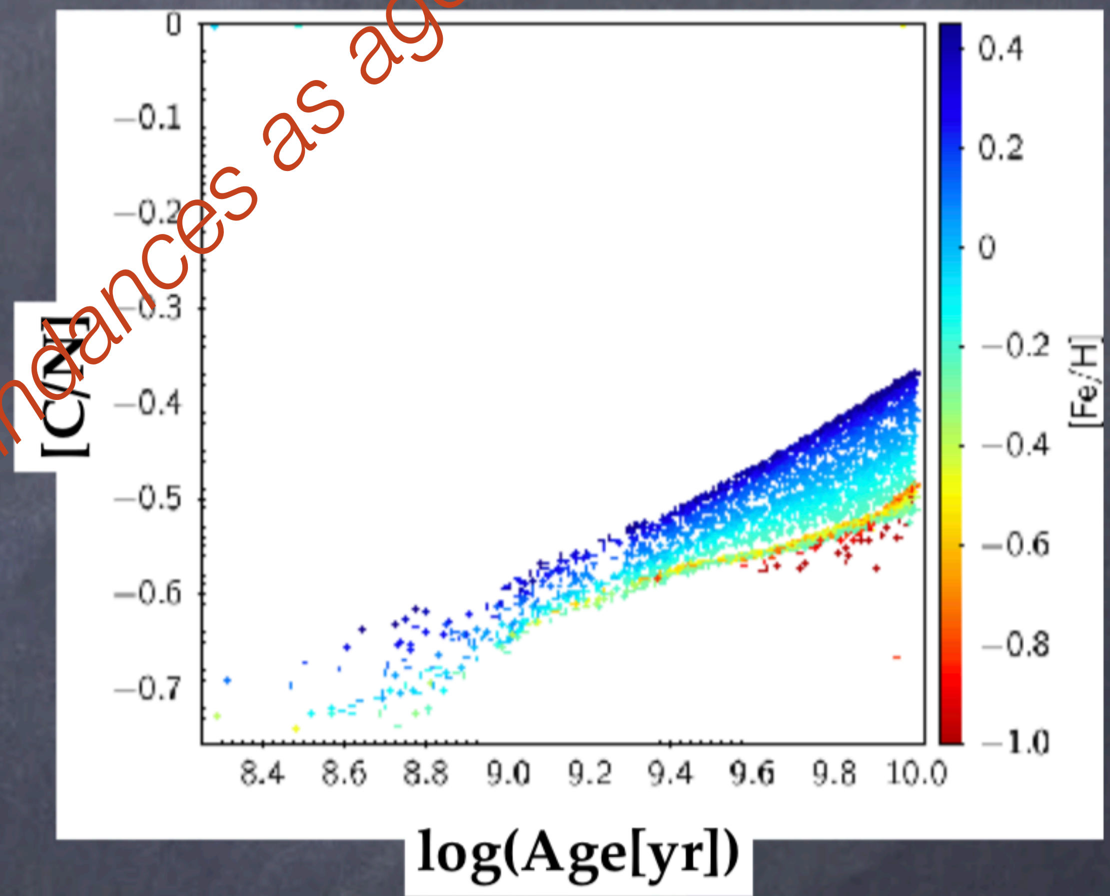

Clump stars

Warning on the use of abundances as age indicator

Lagarde et al 2018

Fields stars (374 giants with C, N abundances)

(open and globular) clusters

VS

BGM simulation of GES survey with **standard stellar evolution models**

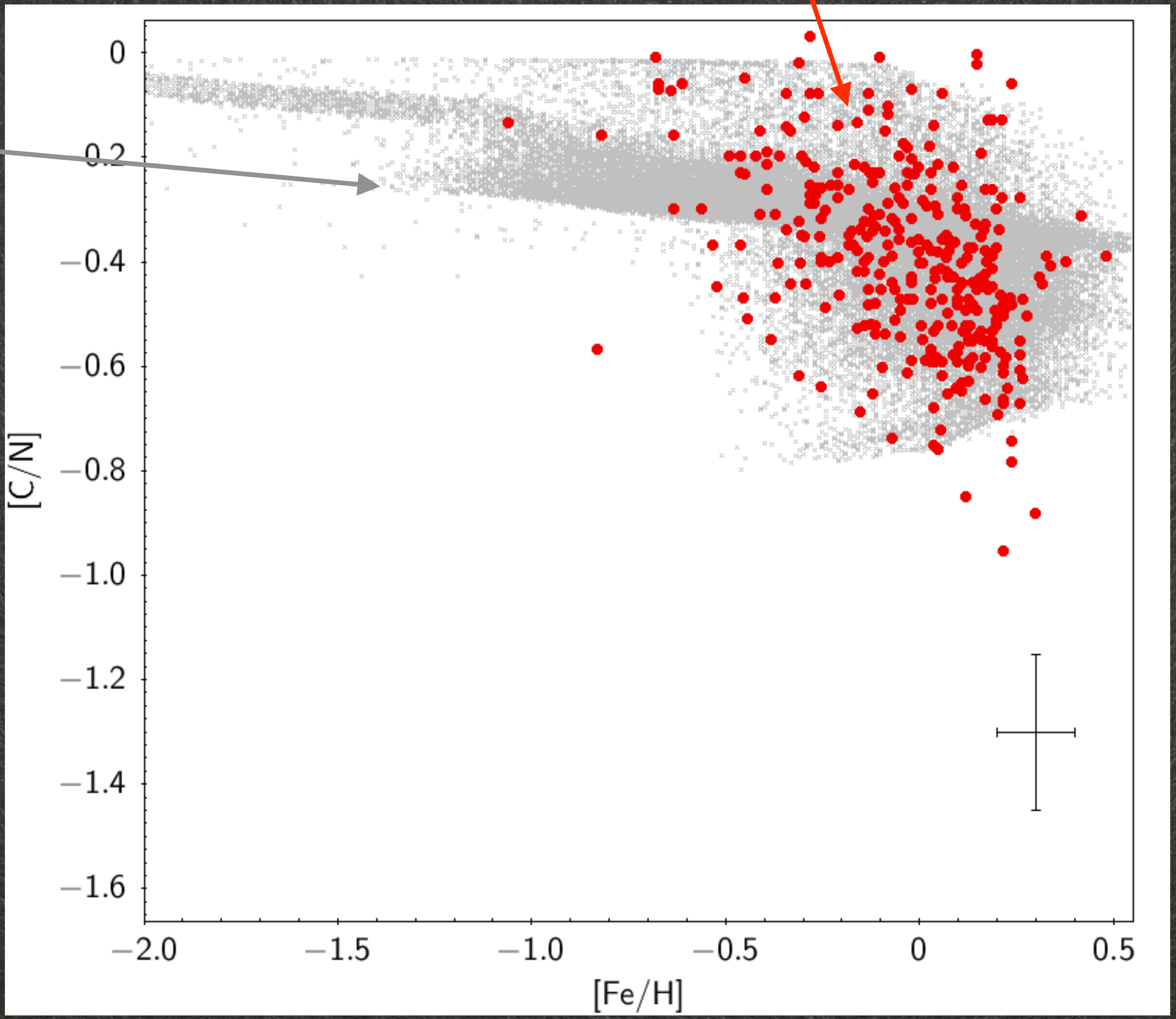

Lagarde et al 2018.

VS

Fields stars (374 giants with C, N abundances)

(open and globular) clusters

BGM simulation of GES survey with **thermohaline stellar evolution models**

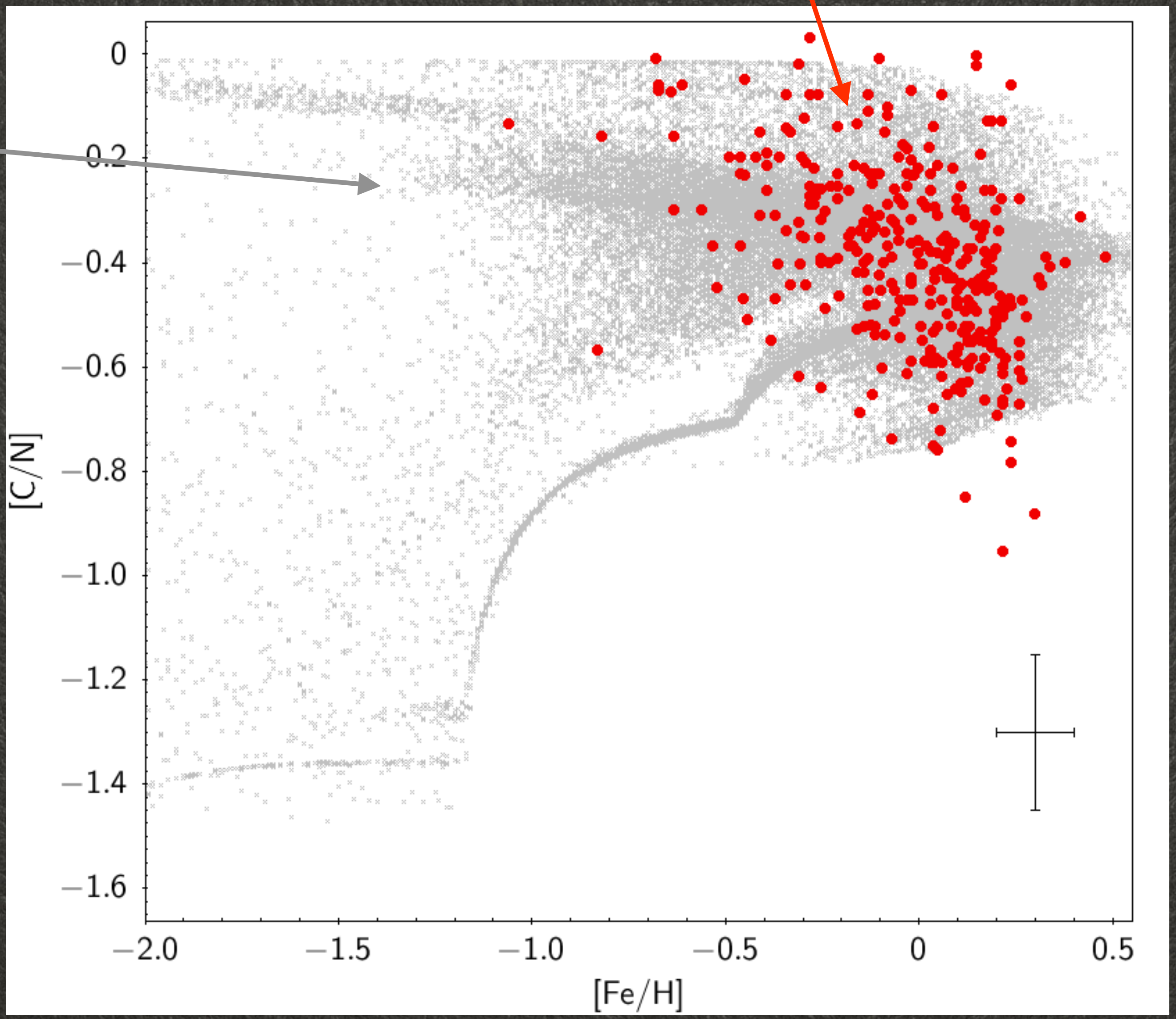

No evidence to constrain the effect of thermohaline mixing at low-Z (where it is more effective)

Lagarde et al 2018

Fields stars (374 giants with C, N abundances)

(open and globular) clusters

VS

BGM simulation of GES survey with **standard stellar evolution models**

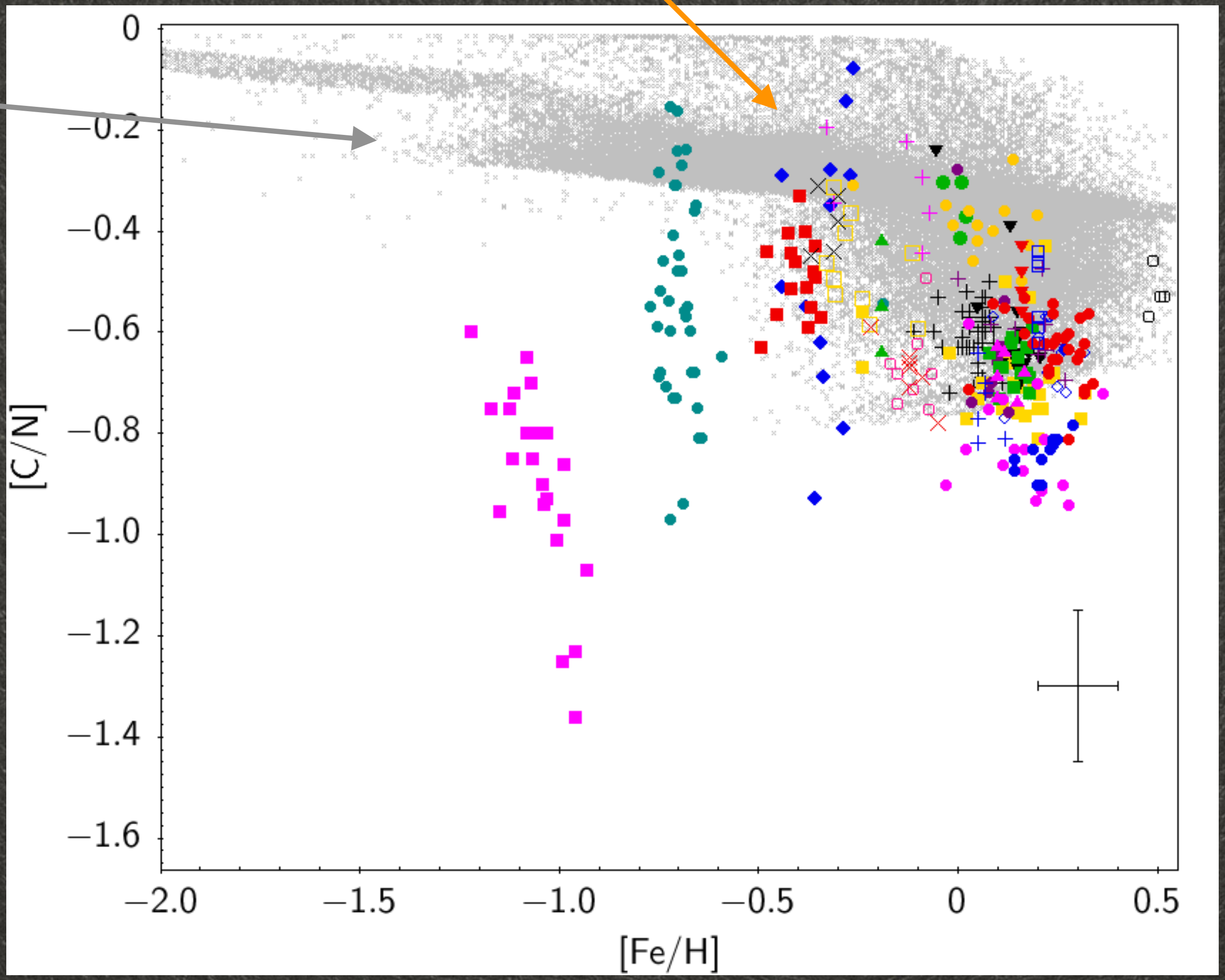

Lagarde et al 2018 subm.

Fields stars (374 giants with C, N abundances)

(open and globular) clusters

VS

BGM simulation of GES survey with **thermohaline stellar evolution models**

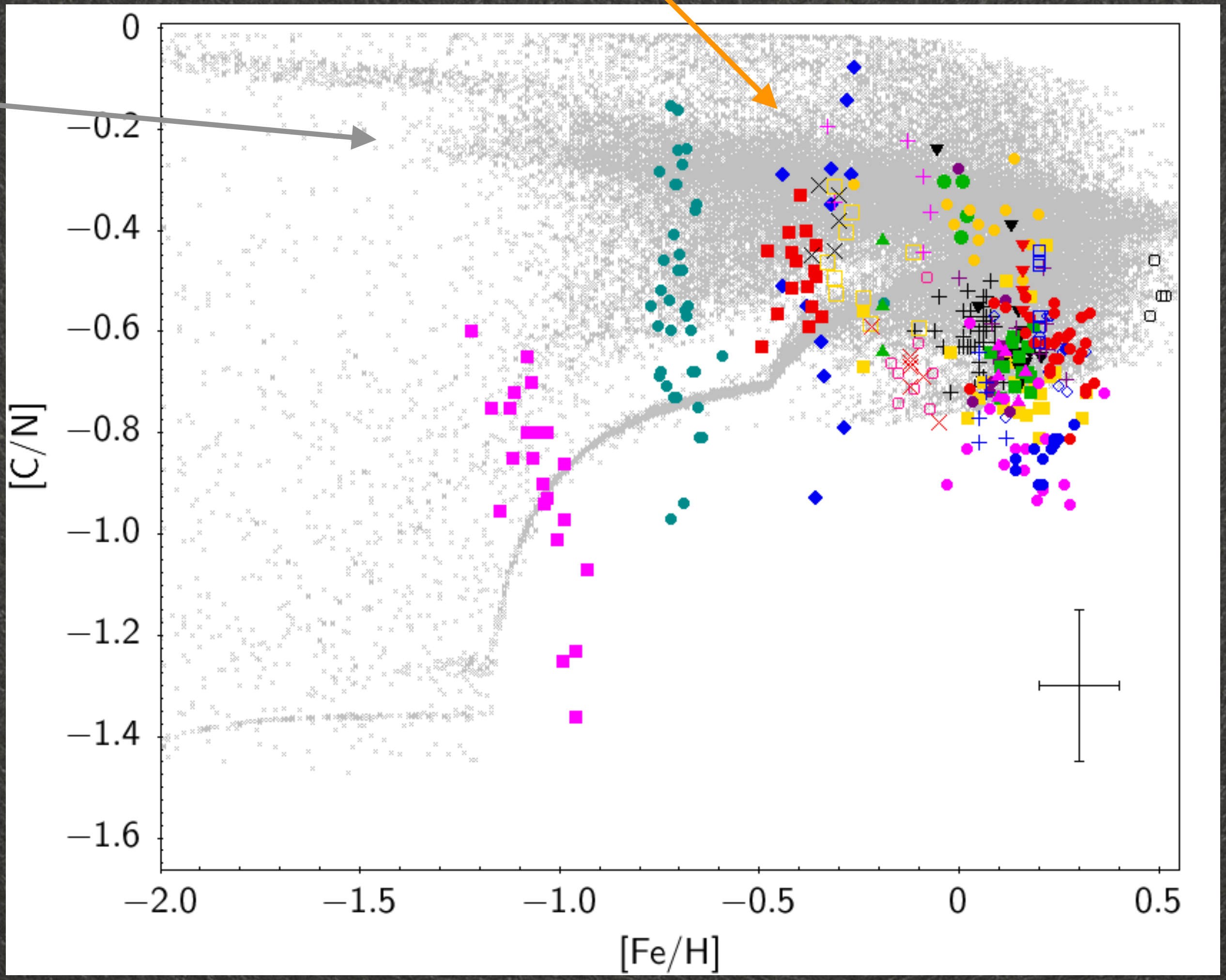

Same behaviors of [**C/N] with [Fe/H]** are observed in the DR14 of APOGEE data !!

Asteroseismic surveys

Study the stellar pulsation modes

⟶ Properties of stellar interiors

+K2

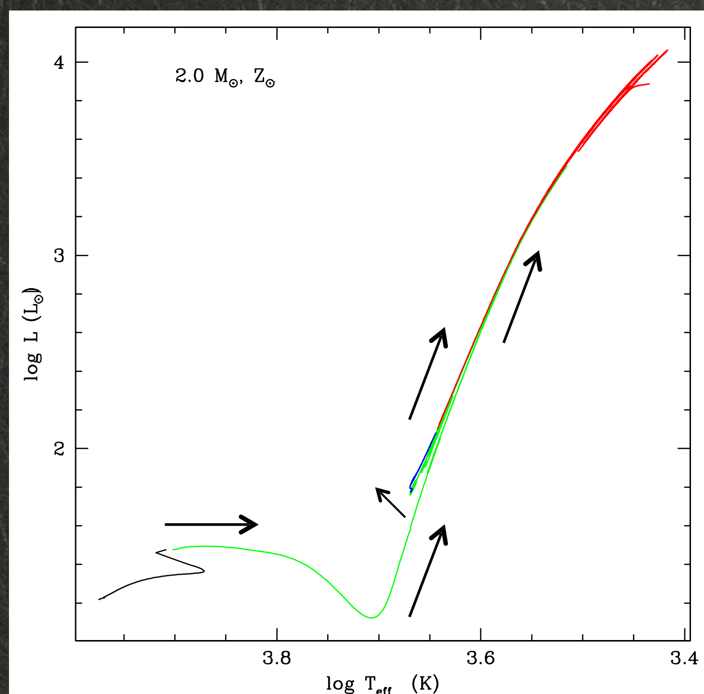

Mosser et al. (2014)

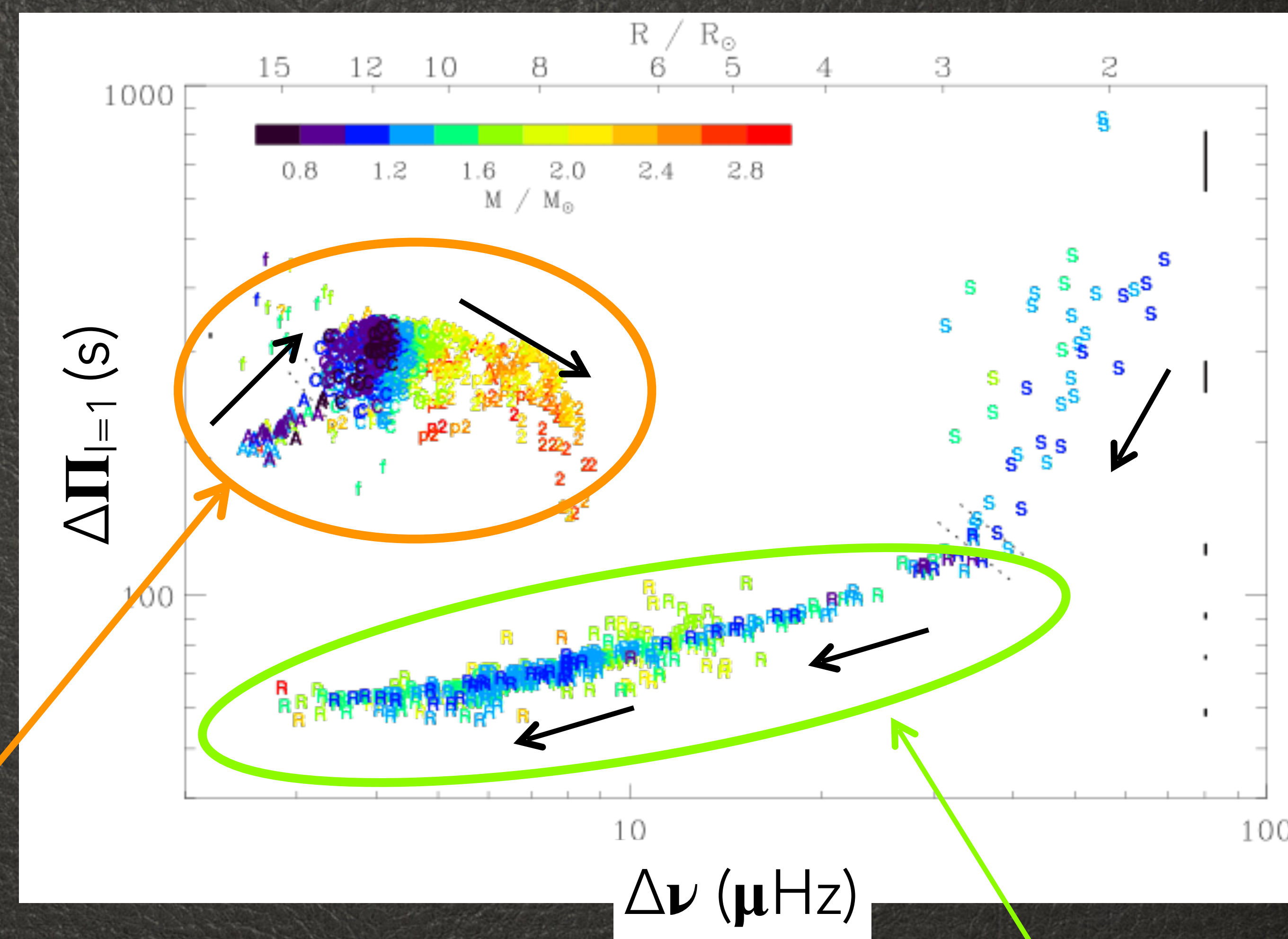

He-burning stars

Red-giant stars

Courtesy of Nadège Lagarde

Lagarde et al 2017

Astero-seismic parameters

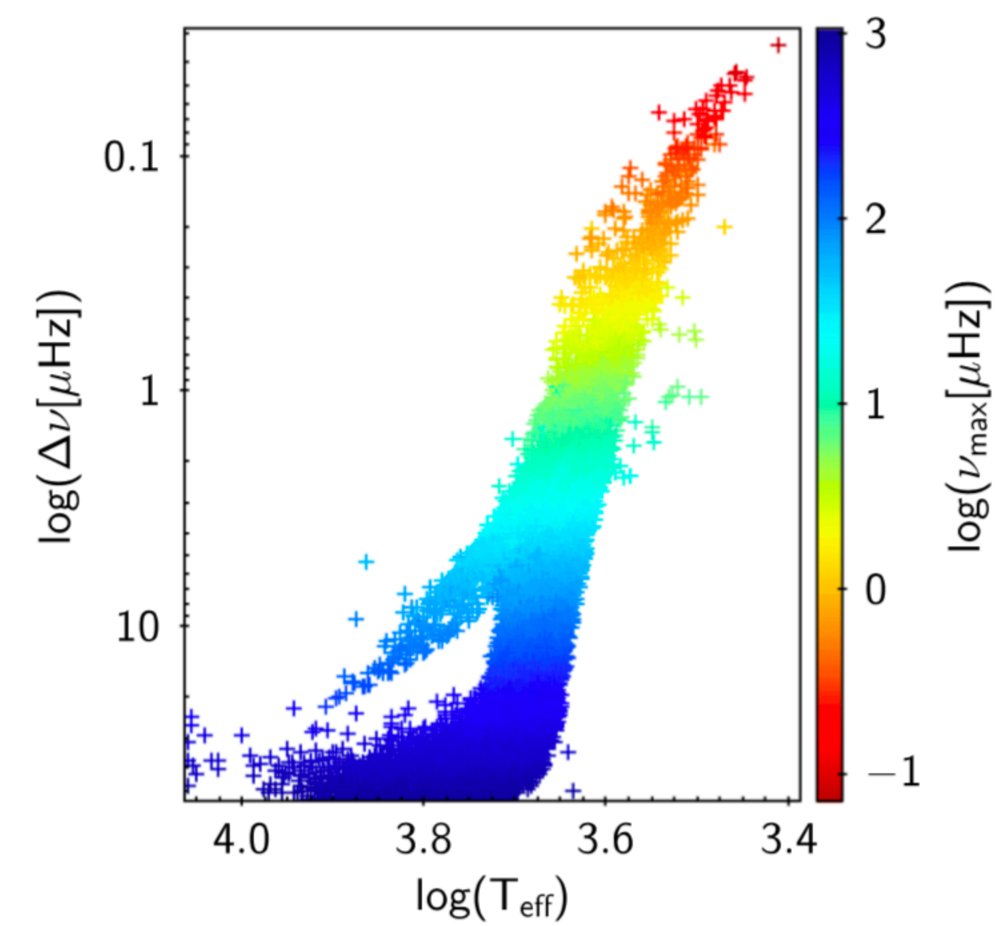

Fig. 2. Large separation, $\Delta\nu$, as a function of the effective temperature, $T_{\rm eff}$, for synthetic population computed with the BGM. Colours indicate the $\nu_{\rm max}$, the frequency at which the power spectrum is maximum.

Analysis of APOKASC on-going

BGM-Fast

- Weighted implementation of Besancon Galaxy Model to explore large surveys and fit multi-parameter models.
- 10^3 to 10^4 faster than BGM
- Combined with ABC (approximate bayesian computation)
- Applied on Gaia data with parallaxes (not using distances), Mor et al, A&A 620, A79 (2018)

BGM FASt:

the weight function applied nowadays to the thin disc

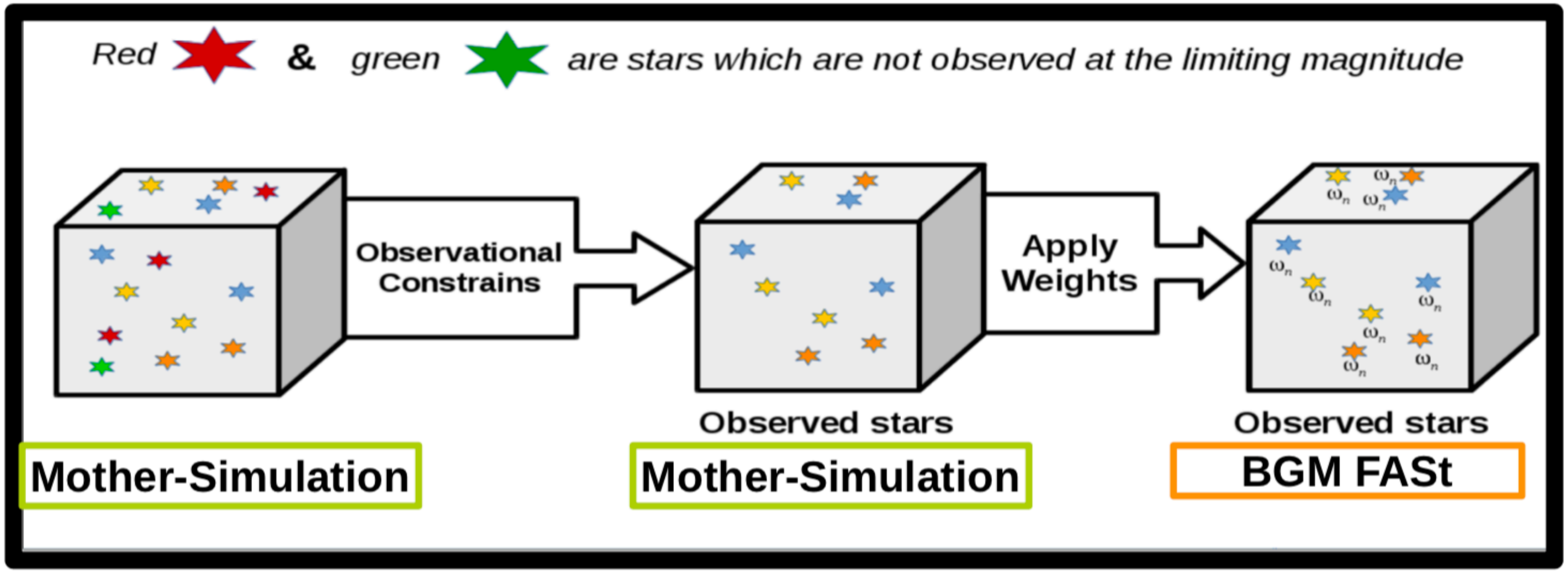

$$w_i(\Delta\tau, \Delta M, \Delta\bar{x}) \approx \frac{\int_{\Delta} \frac{\Sigma_{\odot}^{i,\Delta} \cdot \psi_{\odot}^{i}(\tau)}{\mathcal{H}_i(\tau)} \cdot \mathcal{R}_i(\tau, \bar{x}) \cdot \xi_i(M) \cdot M \;\; d\tau dM\, d\bar{x}}{\int_{\Delta} \frac{\Sigma_{\odot}^{i,\Delta} \;\; \psi_{\odot}^{i}(\tau)}{\mathcal{H}_i(\tau)} \cdot \mathcal{R}_i(\tau, \bar{x}) \cdot \xi_i(M) \cdot M \;\; d\tau dM\, d\bar{x}}$$

BGM FASt:
building the weight function

$$\left[\,\cdot\,\right]_\Delta = \mathcal{N}_i(\Delta\tau, \Delta M, \Delta Z, \Delta\bar{x}, \Delta[\alpha/Fe]) \approx$$

$$\approx \frac{\displaystyle\int_\Delta \frac{\Sigma^i_\odot \cdot \psi^i_\odot(\tau)}{\mathcal{H}_i(\tau)} \cdot \mathcal{R}_i(\tau,\bar{x}) \cdot \xi_i(M) \cdot M \cdot \mathcal{P}_i(Z|\tau,\bar{x}) \cdot P_i(\alpha|\tau,Z,\bar{x}) \cdot d\tau dM\, dZ\, d\bar{x}\, d\alpha}{\displaystyle\int_\Delta \frac{\Sigma^i_\odot \cdot \psi^i_\odot(\tau)}{\mathcal{H}_i(\tau)} \cdot \mathcal{R}_i(\tau,\bar{x}) \cdot \xi_i(M) \cdot M \cdot \mathcal{P}_i(Z|\tau,\bar{x}) \cdot P_i(\alpha|\tau,Z,\bar{x}) \cdot d\tau dM\, dZ\, d\bar{x}\, d\alpha} \bullet \mathcal{N}_i(\Delta\tau, \Delta M, \Delta Z, \Delta\bar{x}, \Delta[\alpha/Fe])$$

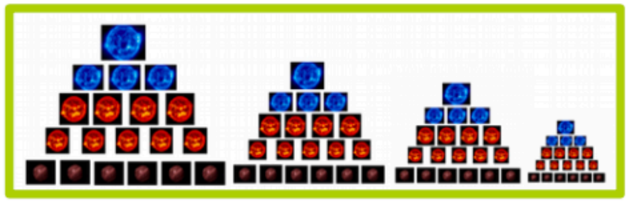

Δ

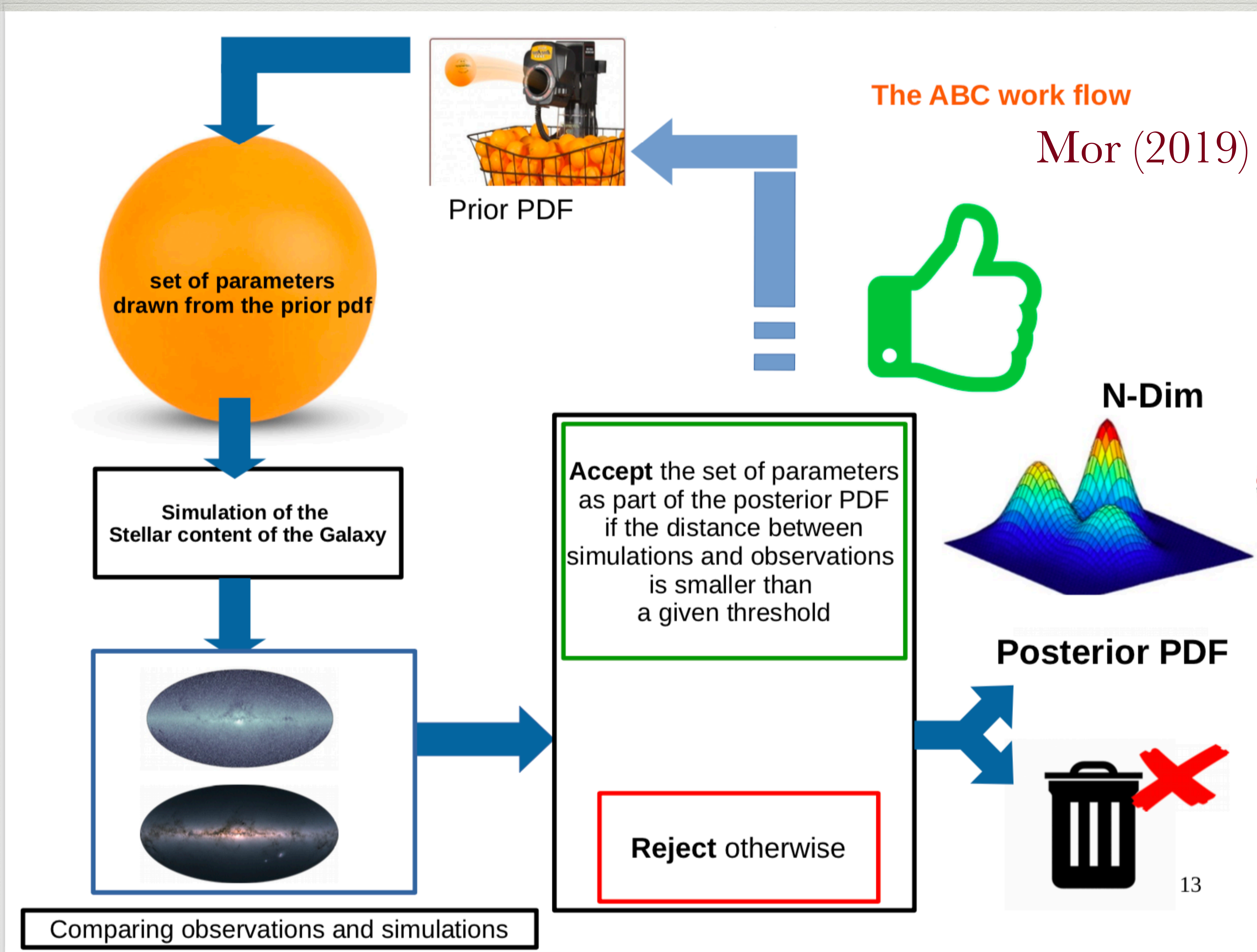
The ABC work flow
Mor (2019)
Prior PDF
set of parameters
drawn from the prior pdf
Simulation of the
Stellar content of the Galaxy
Accept the set of parameters
as part of the posterior PDF
if the distance between
simulations and observations
is smaller than
a given threshold
Reject otherwise
N-Dim
Posterior PDF
Comparing observations and simulations
13

For a parametrized SFH

SFH
Exp

IMF
slopes

Scale
Length

Local
Density

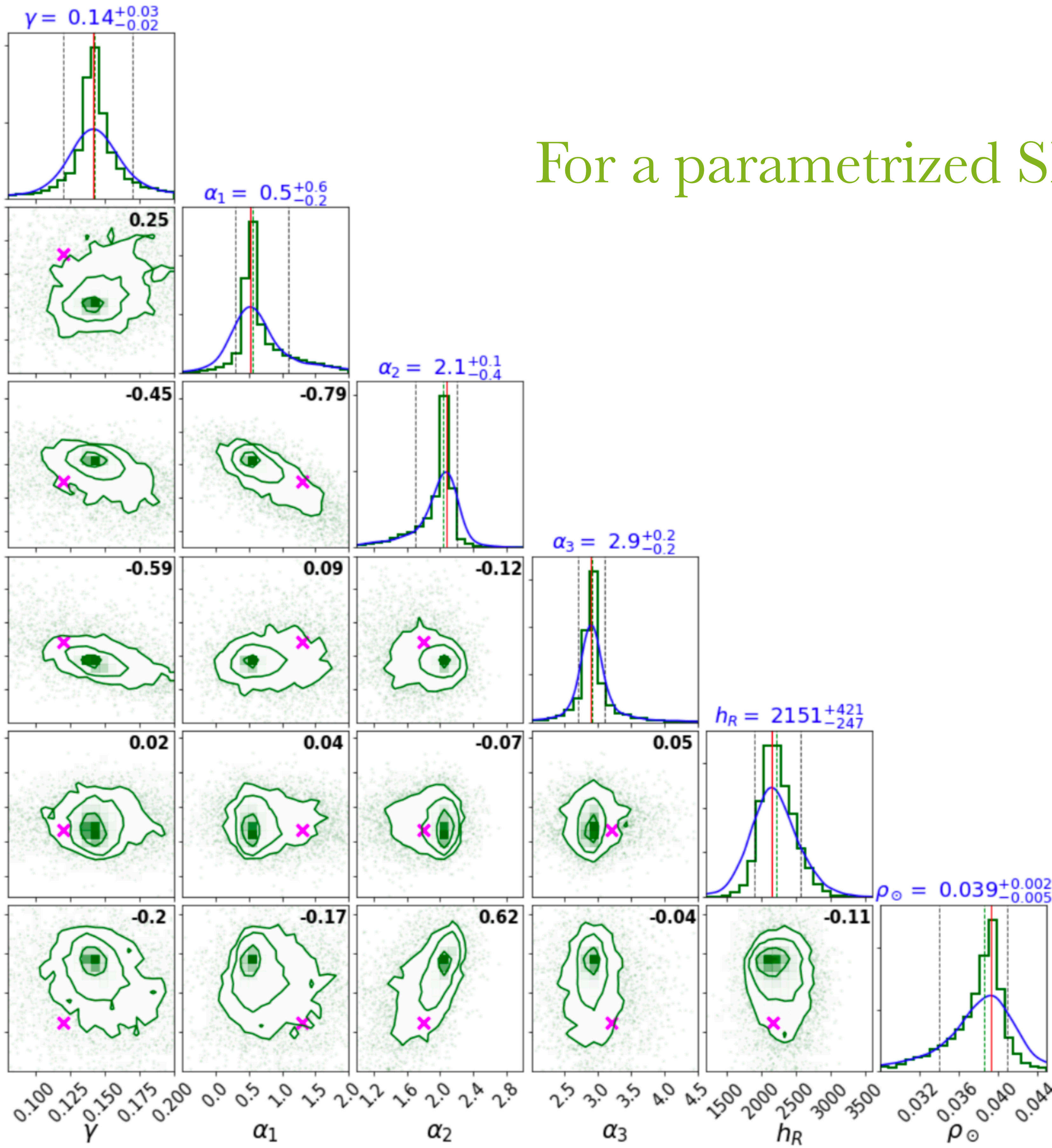

Gaia

Param SFH (exp)

Non param SFH

Pole

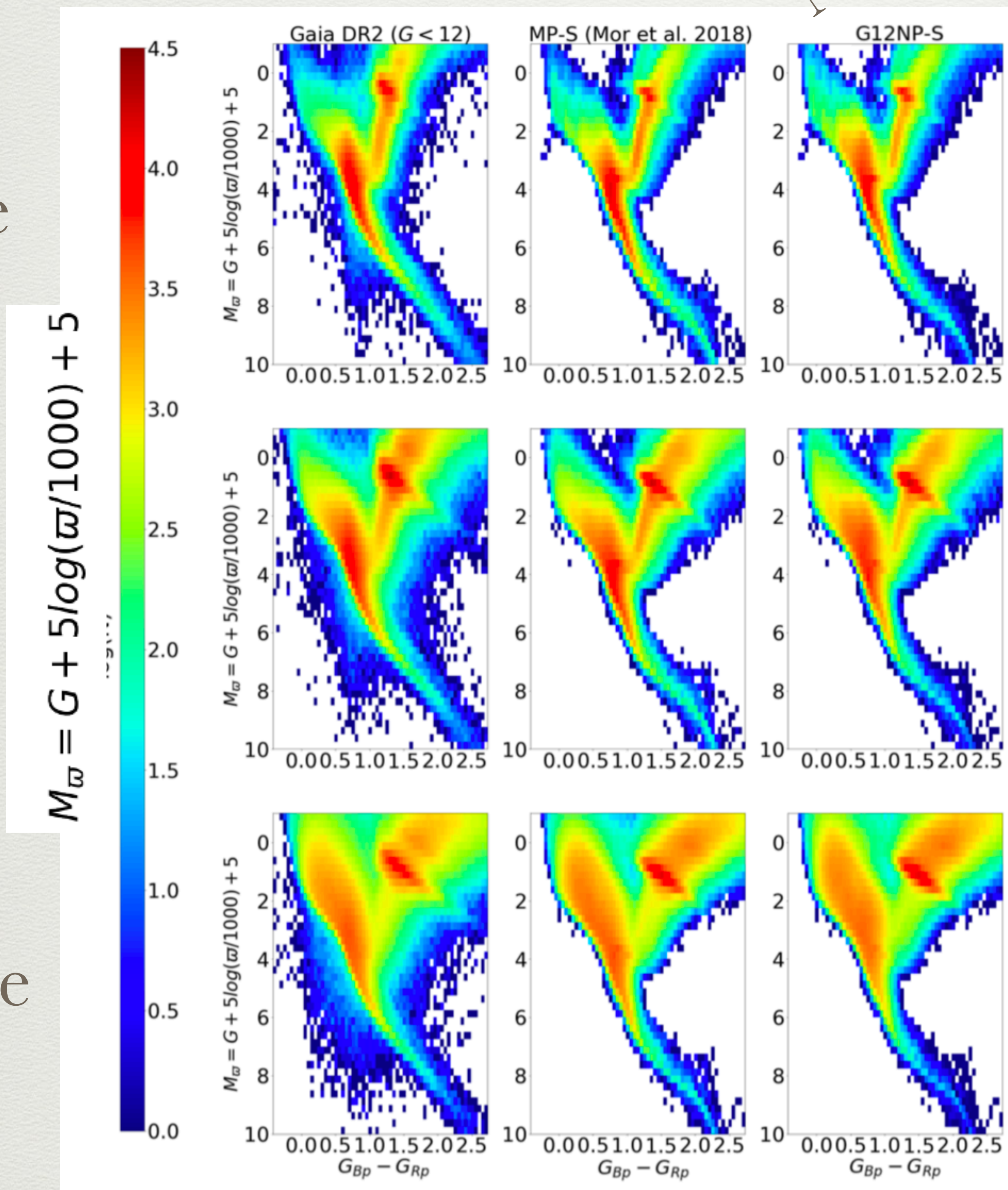

Plane

Non parametric SFH
Improves the fit

IMF

Gaia

Param SFH (exp)

Non param SFH

Pole

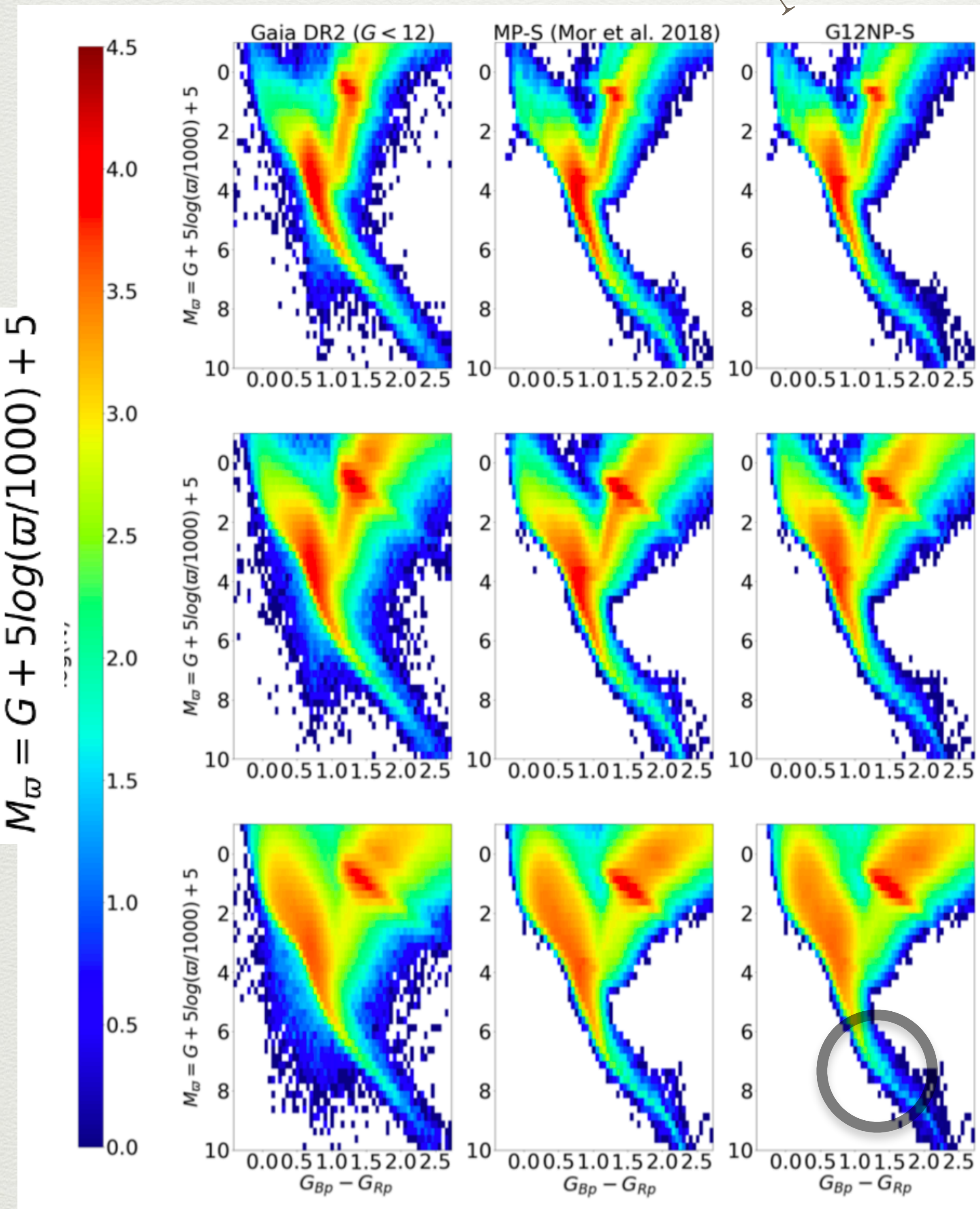

Plane

Non parametric SFH
Improves the fit

IMF

Gaia

Param SFH (exp)

Non param SFH

Pole

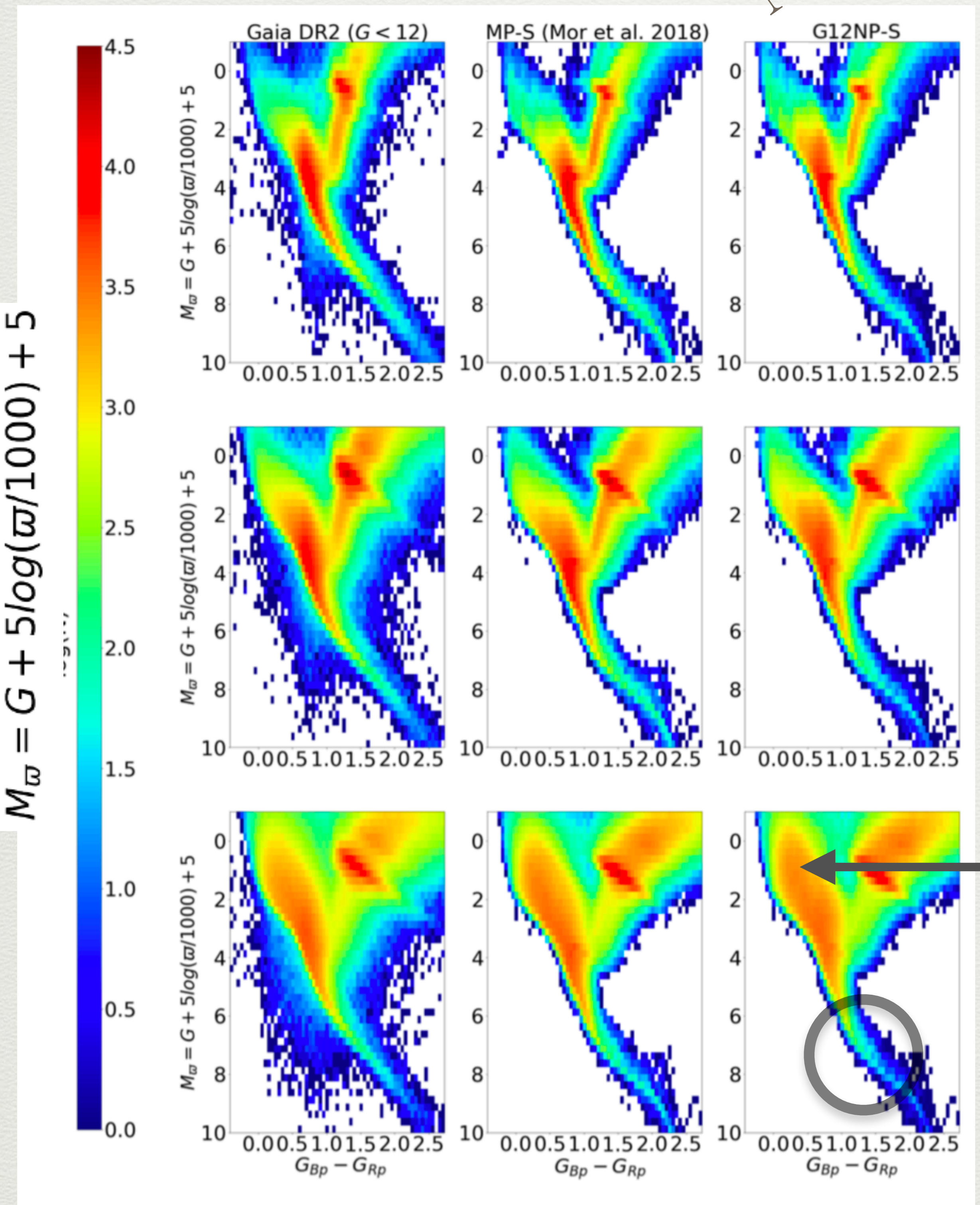

Plane

Non parametric SFH
Improves the fit

IMF

Gaia

Param SFH (exp)

Non param SFH

Pole

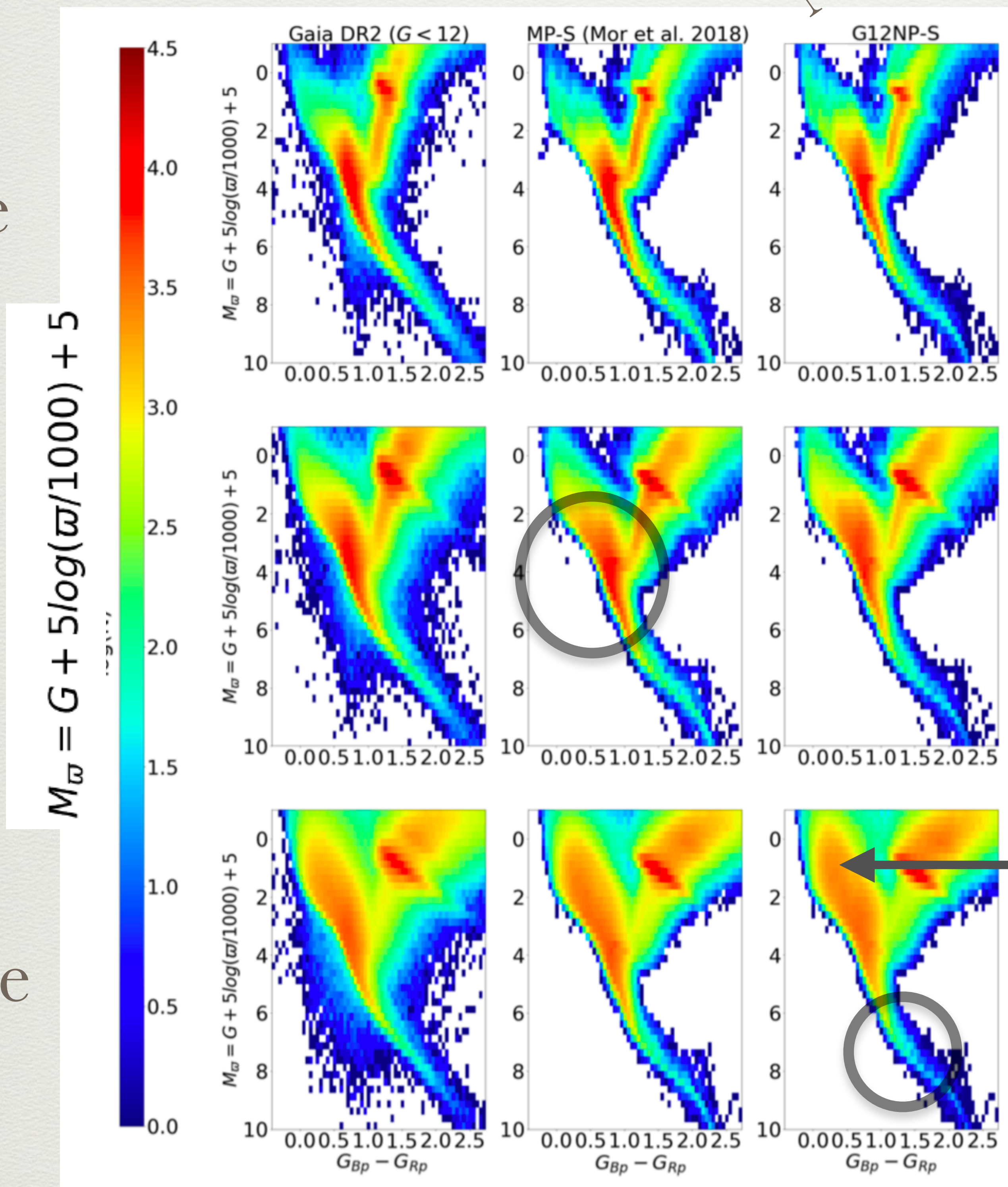

Plane

Non parametric SFH
Improves the fit

IMF

Gaia

Param SFH (exp)

Non param SFH

Pole

Plane

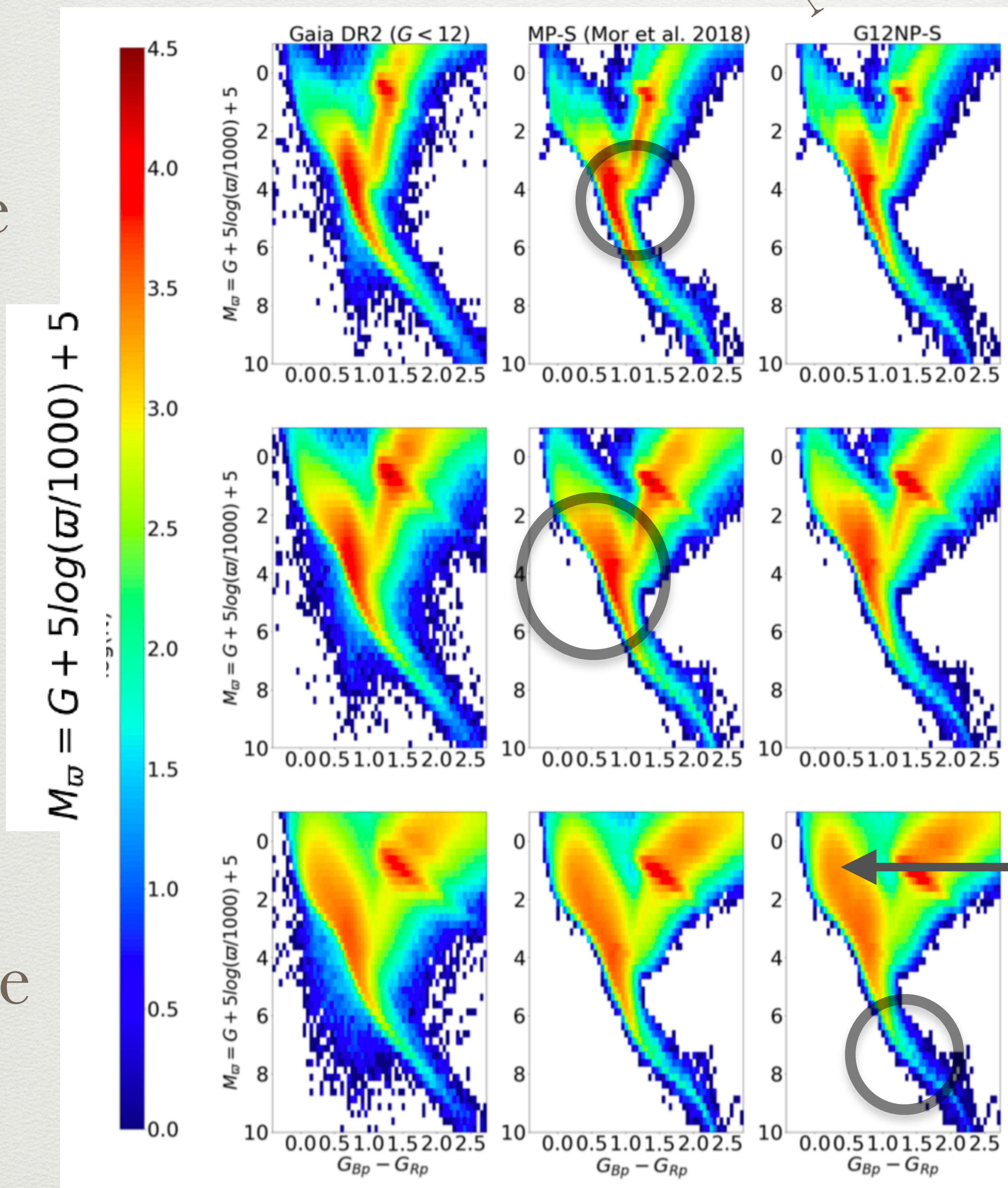

Non parametric SFH
Improves the fit

IMF

Gaia

Param SFH (exp)

Non param SFH

Pole

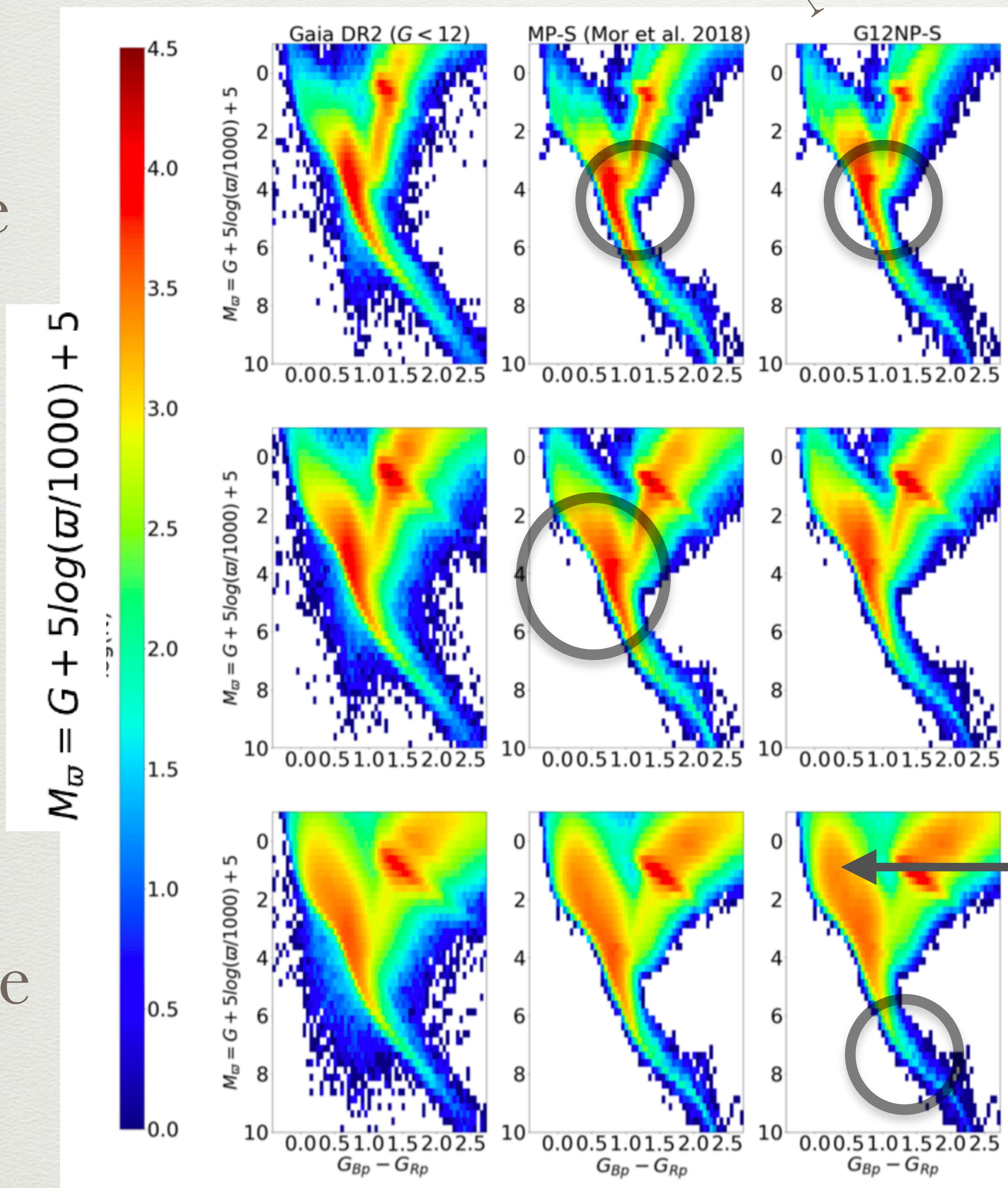

Plane

Non parametric SFH
Improves the fit

IMF

Gaia

Param SFH (exp)

Non param SFH

Pole

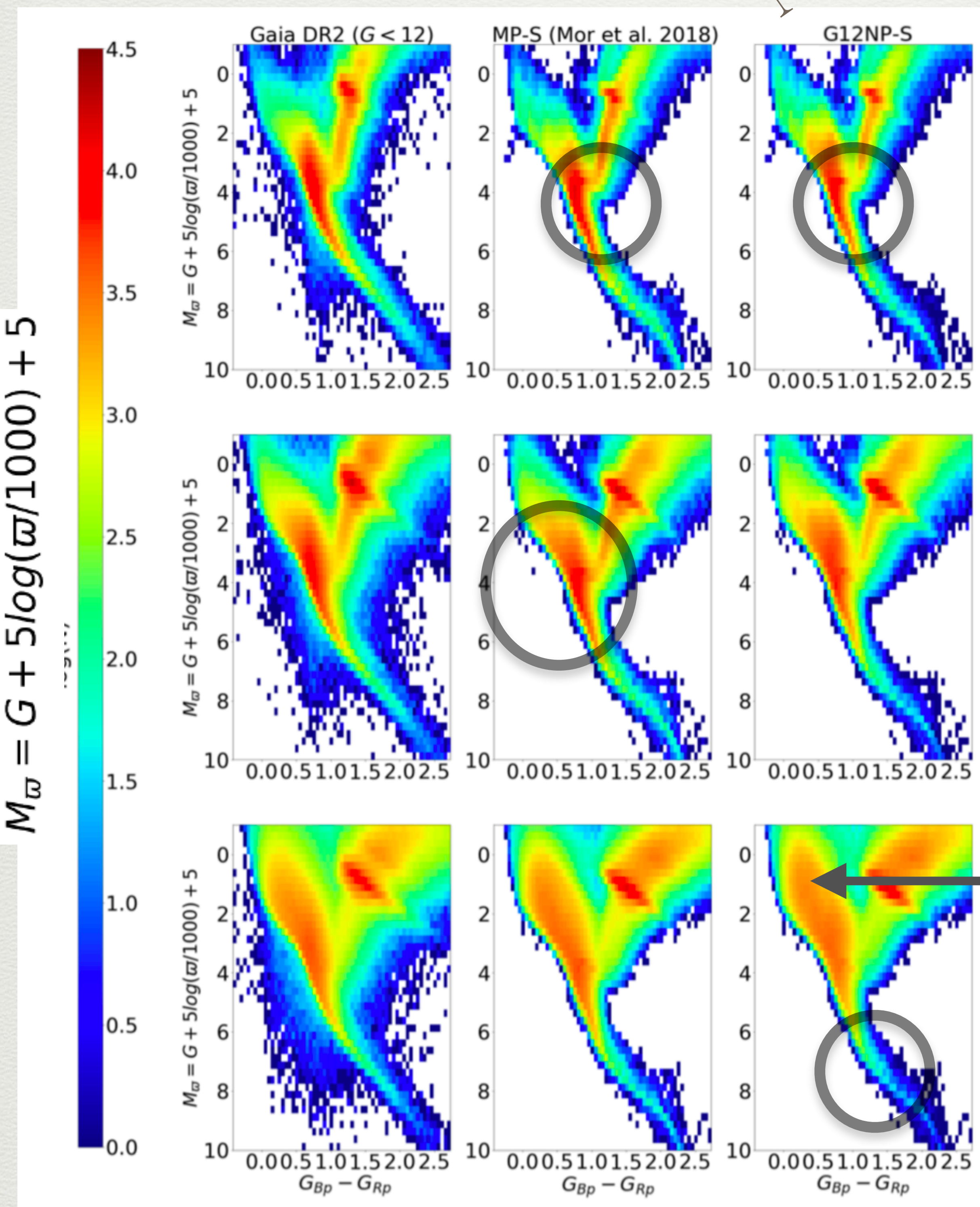

Plane

Non parametric SFH
Improves the fit

IMF

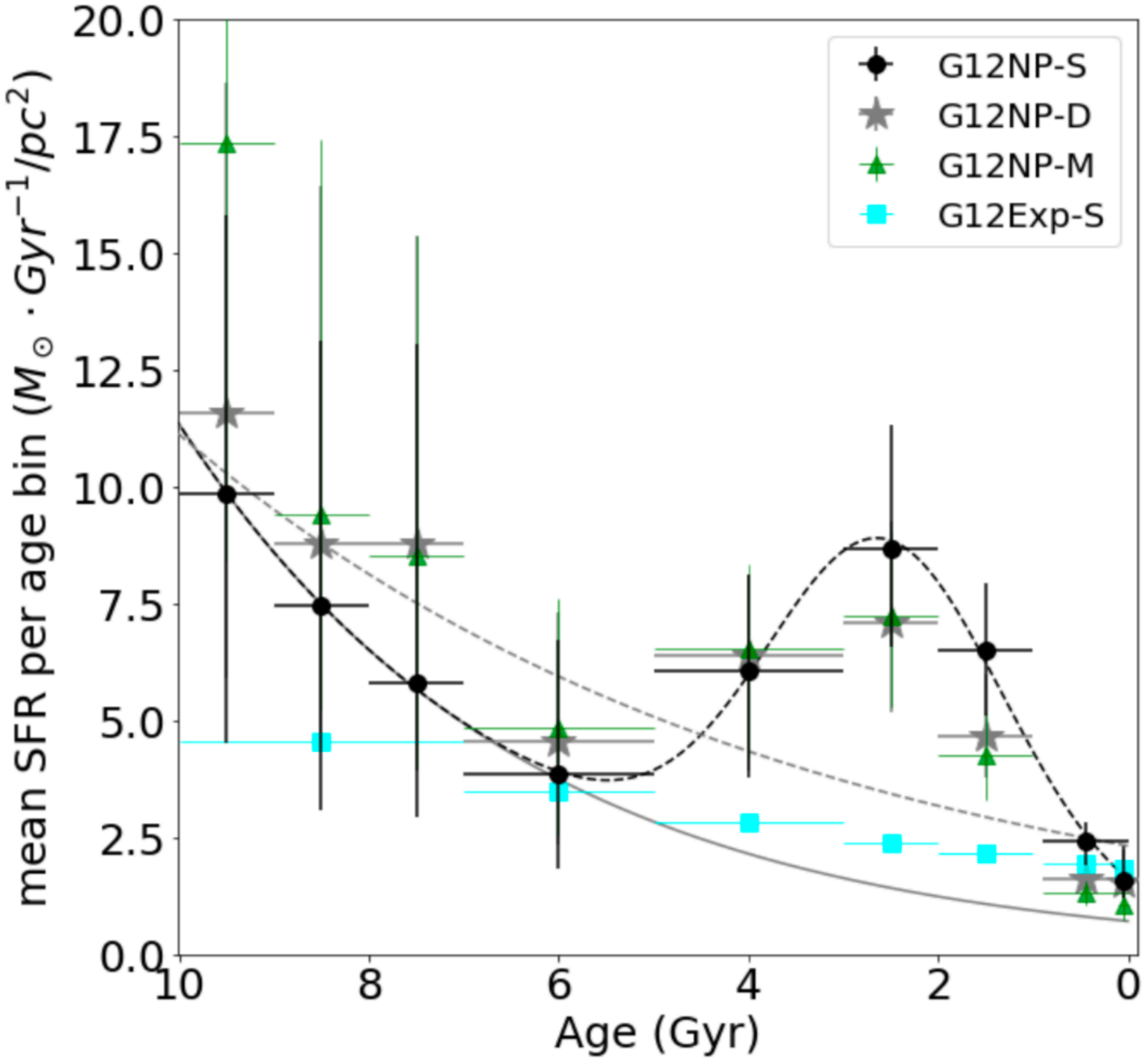

Fig. 2. Most probable values of the mean SFR for the age bin obtained from the posterior PDF. The vertical error bars indicate the 0.16 and 0.84 quantiles of the posterior PDF. The horizontal error bars indicate the size of the age bin. The grey and black dashed lines are, respectively, an exponential function and a distribution formed by a bounded exponential plus a Gaussian, fitted to the G12NP-S results. The grey solid line is the exponential part of this exponential plus Gaussian fit. See Table 2 for details of the SFH and extinction maps used.

Not parametric SFH

Mor et al, 2019,

A&A 624, L1 (2019)

Using Gaia DR2

G<12 mag

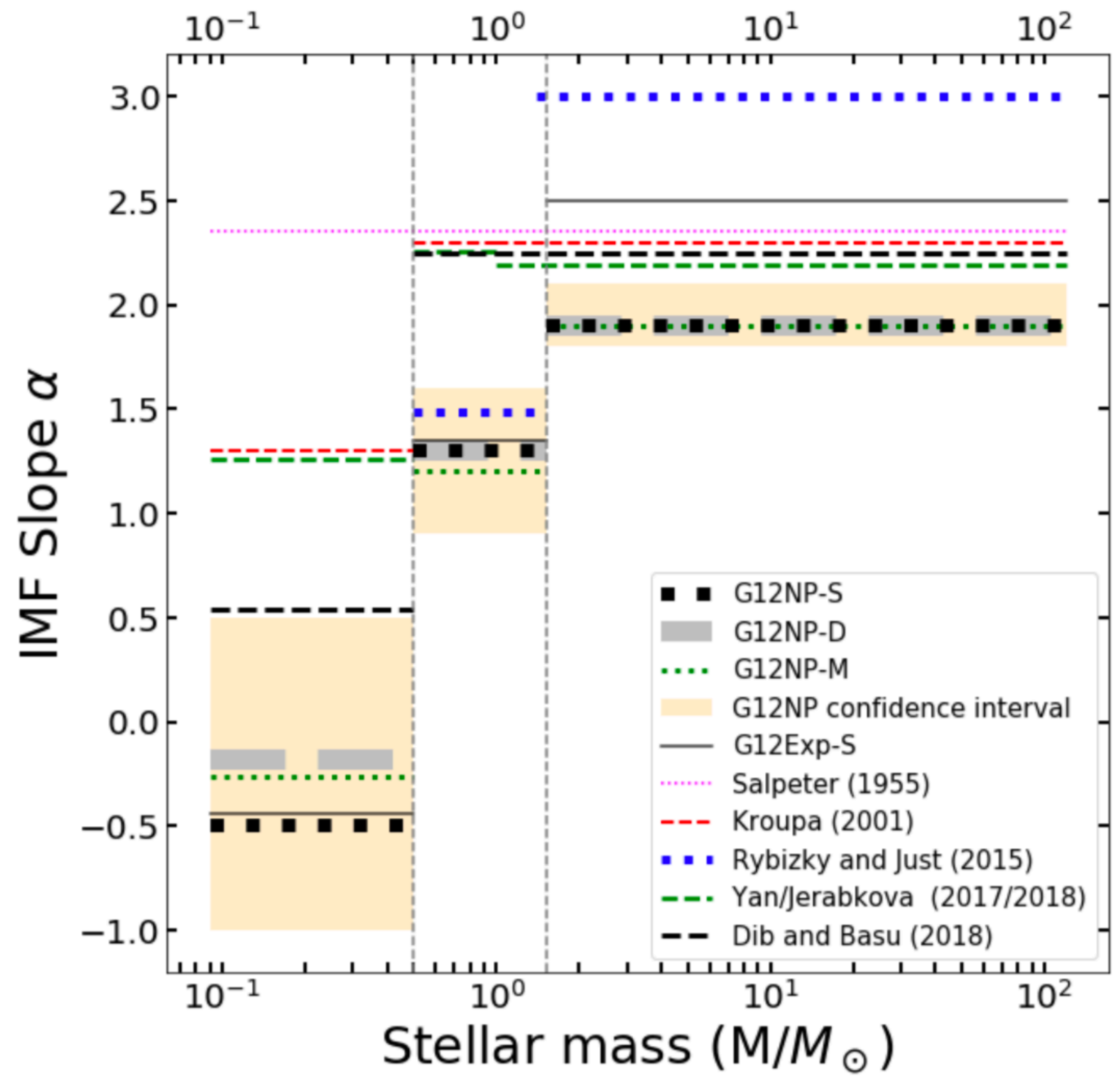

Fig. 3. Values of the slopes of the IMF obtained in this work together with a compilation of results in the literature. The dotted vertical lines indicate the mass limits of the three truncated power-law IMF that we adopt here ($x_1 = 0.5$ and $x_2 = 1.53$). See Table 2 for details on the SFH and extinction maps used.

IMF slopes

Improving extinction modelling

- Stilism approach: Lallement et al 2019, based on DR2 distances and 2MASS, whole sky, d<4 kpc
- Marshall et al (2006) approach (in plane), suitable for the bulge

Improving extinction modelling

- Stilism approac
DR2 distances a

- Marshall et al (2
for the bulge

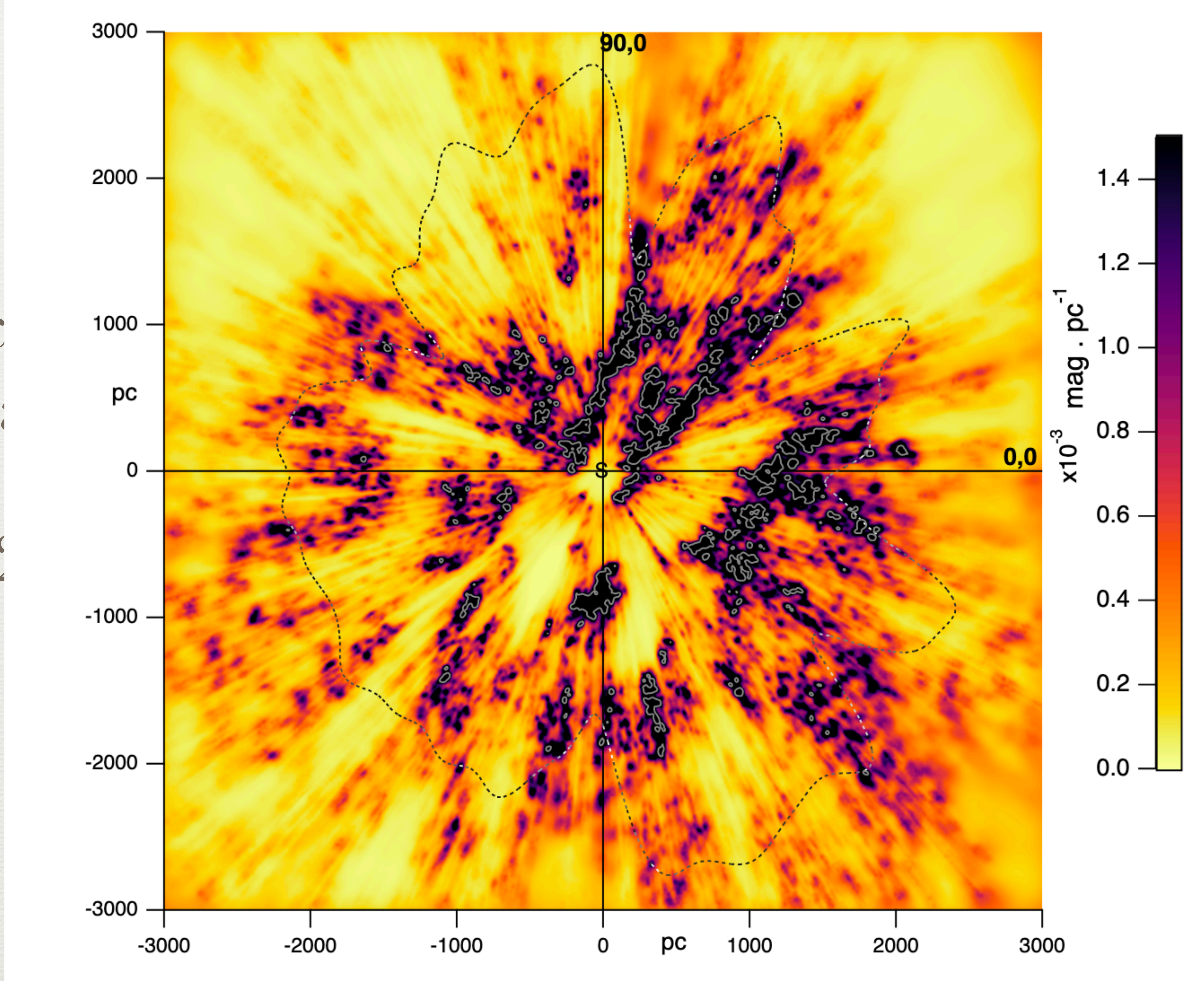

Improving extinction modelling

- Stilism approach: Lallement et al 2019, based on DR2 distances and 2MASS, whole sky, d<4 kpc
- Marshall et al (2006) approach (in plane), suitable for the bulge

Tycho 2 vs Model predictions with different extinction maps

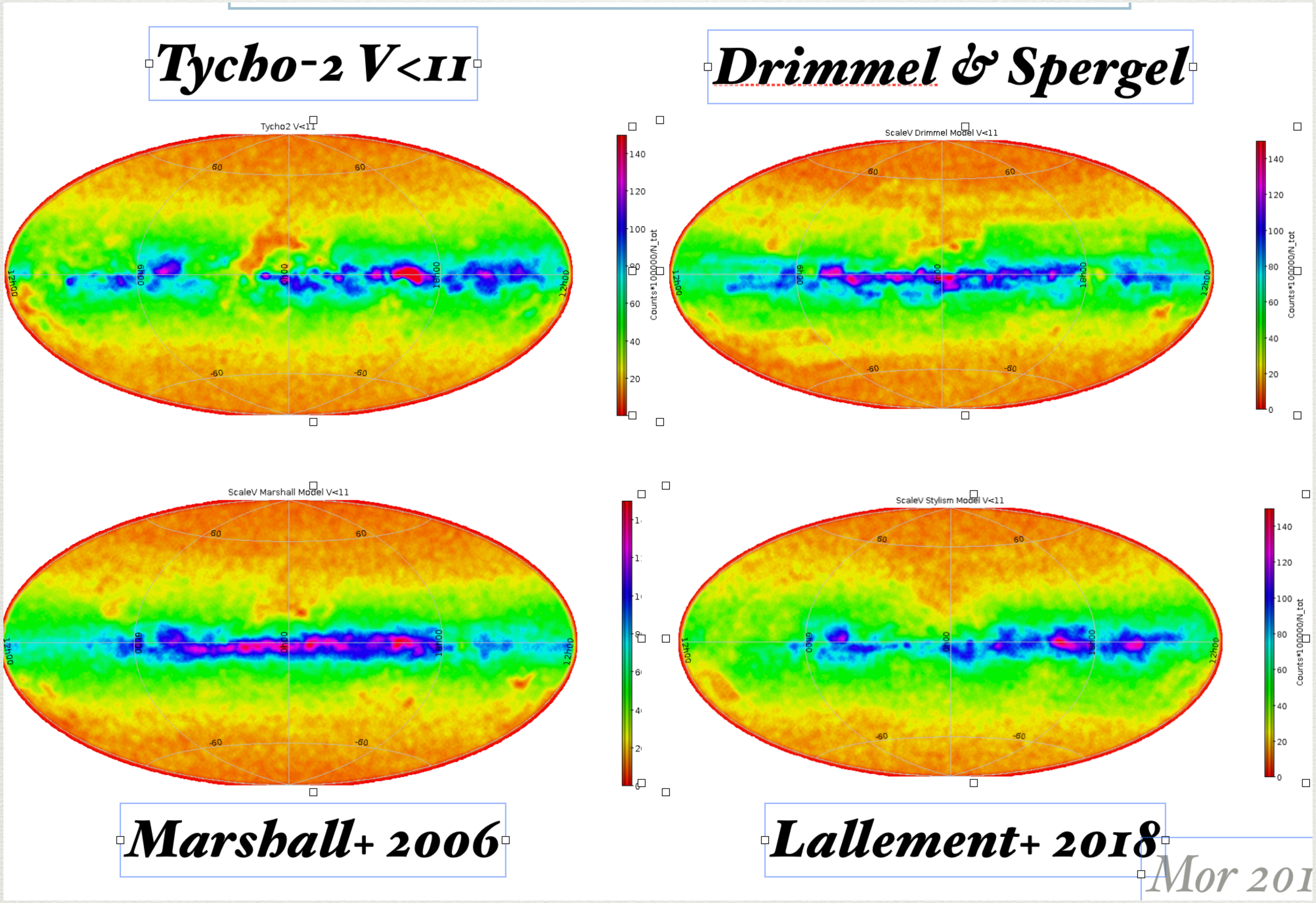

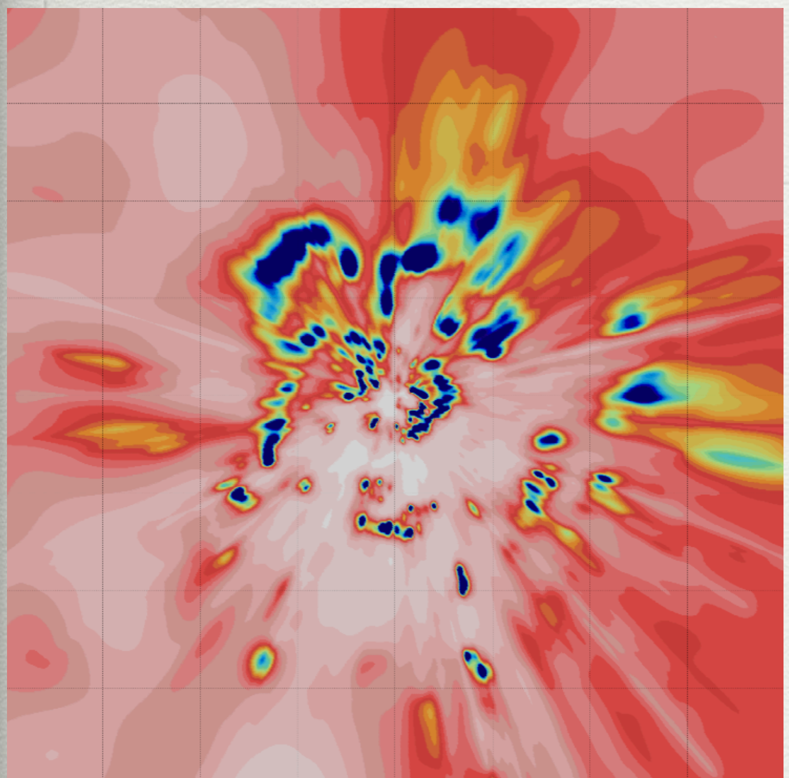

Lallement et al, 2014
Capitanio et al (2017): New map up to 2 kpc

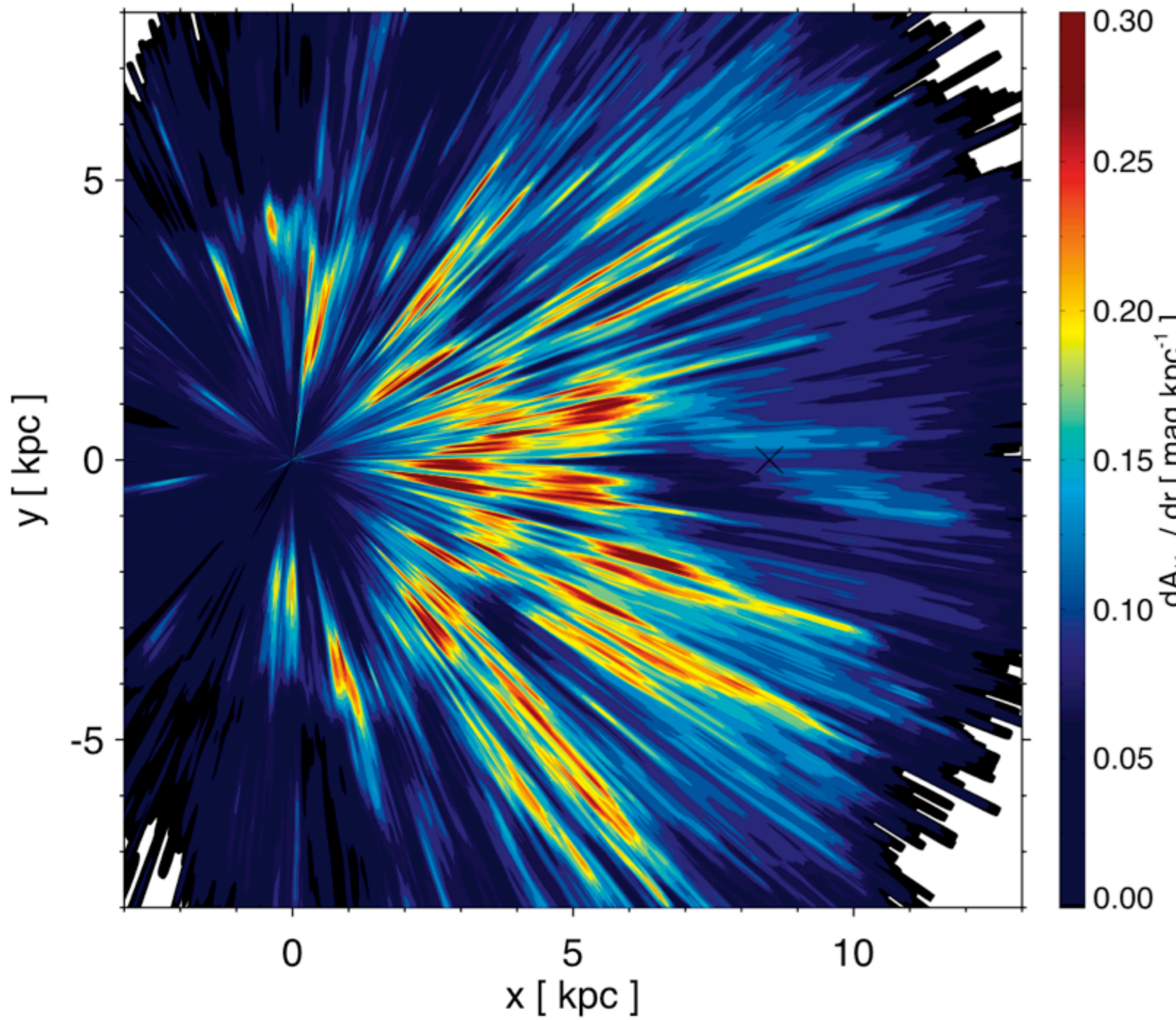

Marshall et al., 2006

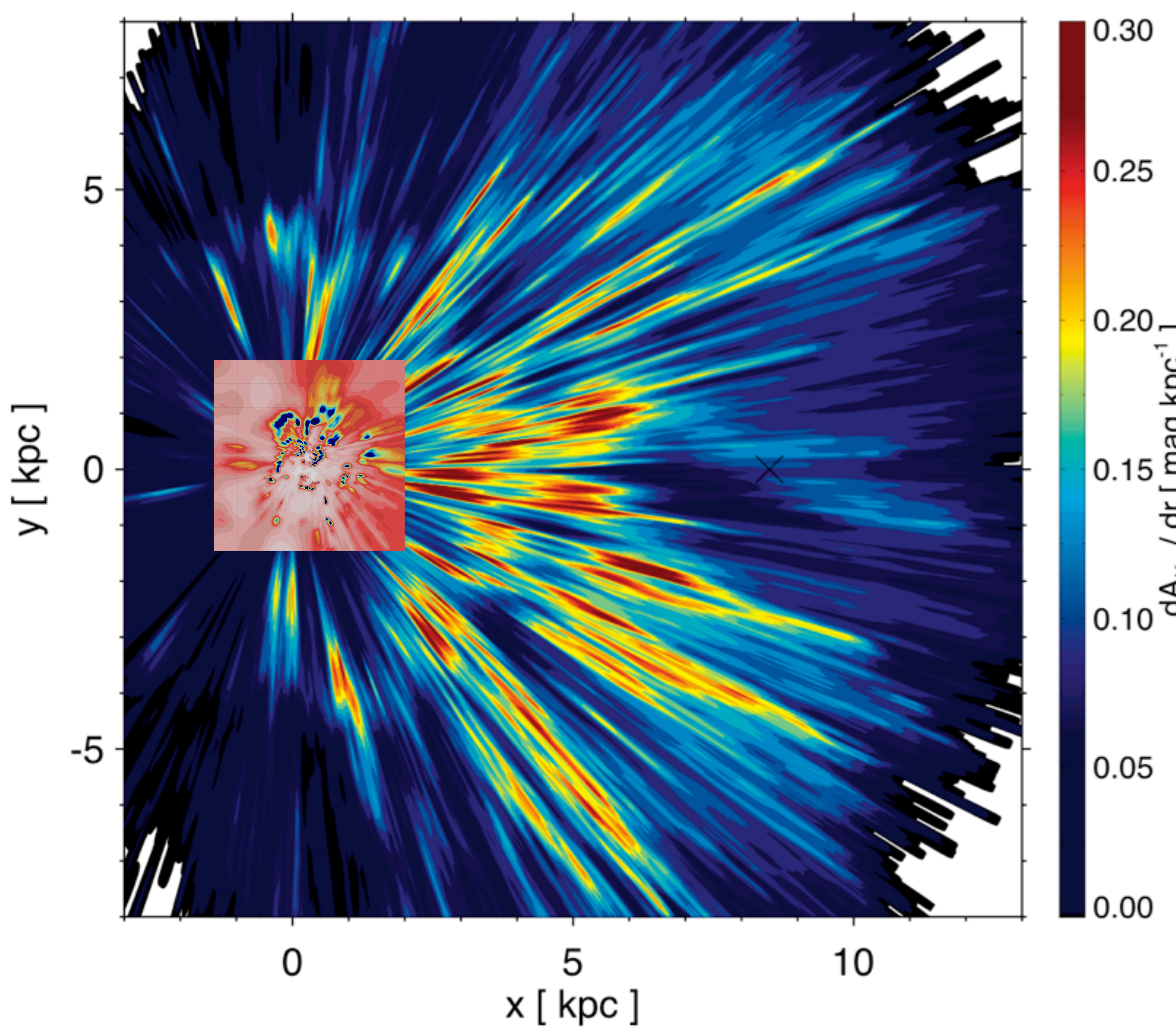

Lallement et al, 2014
Capitanio et al (2017): New map up to 2 kpc

Marshall et al., 2006

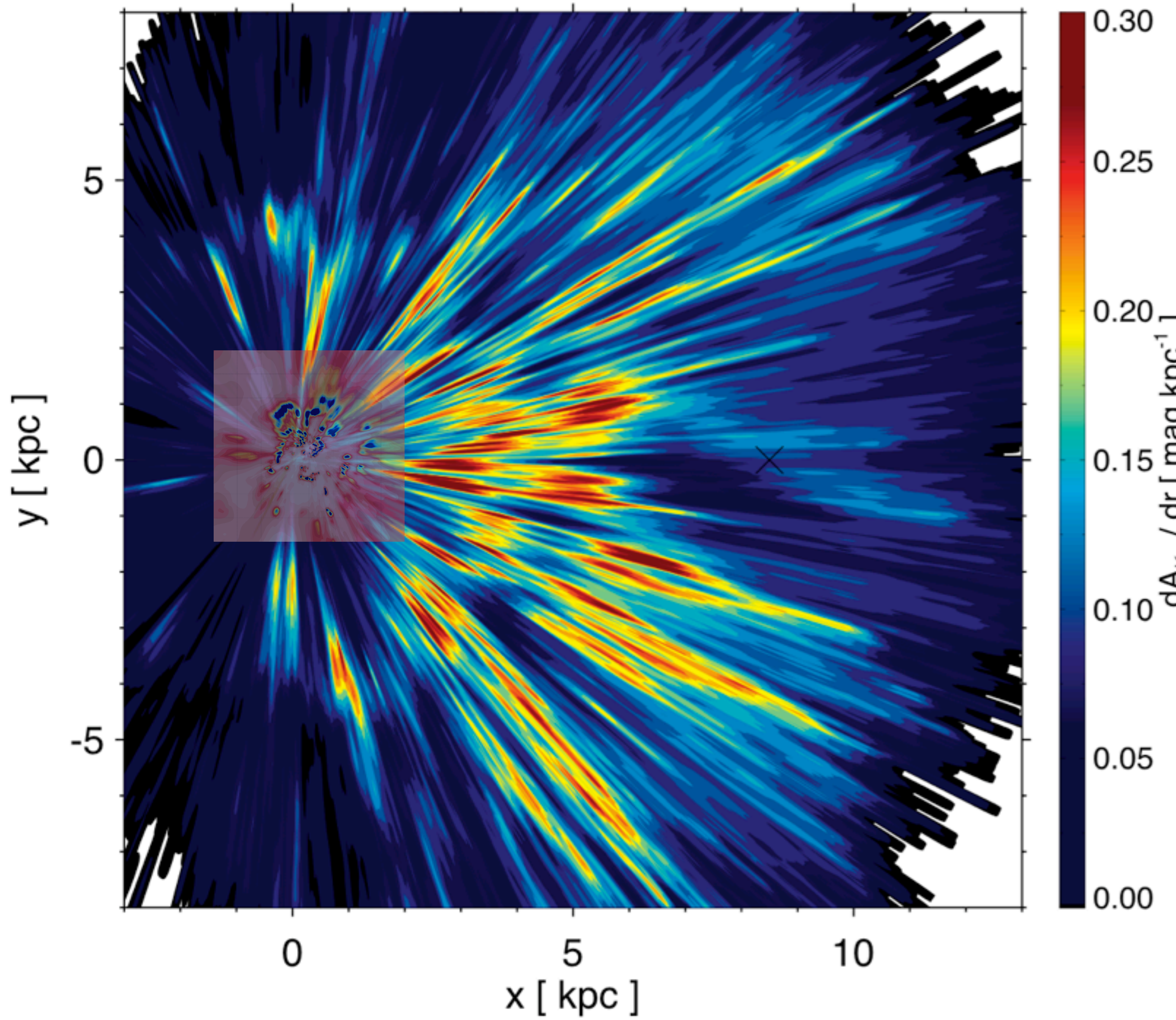

Lallement et al, 2014
Capitanio et al (2017): New map up to 2 kpc

Marshall et al., 2006

Thin disc kinematics

- Dynamically, self-consistent model fit to Gaia DR1
- Robin et al 2017
- Bienaymé et al 2018

Approximate BGM potential with a Stäckel potential

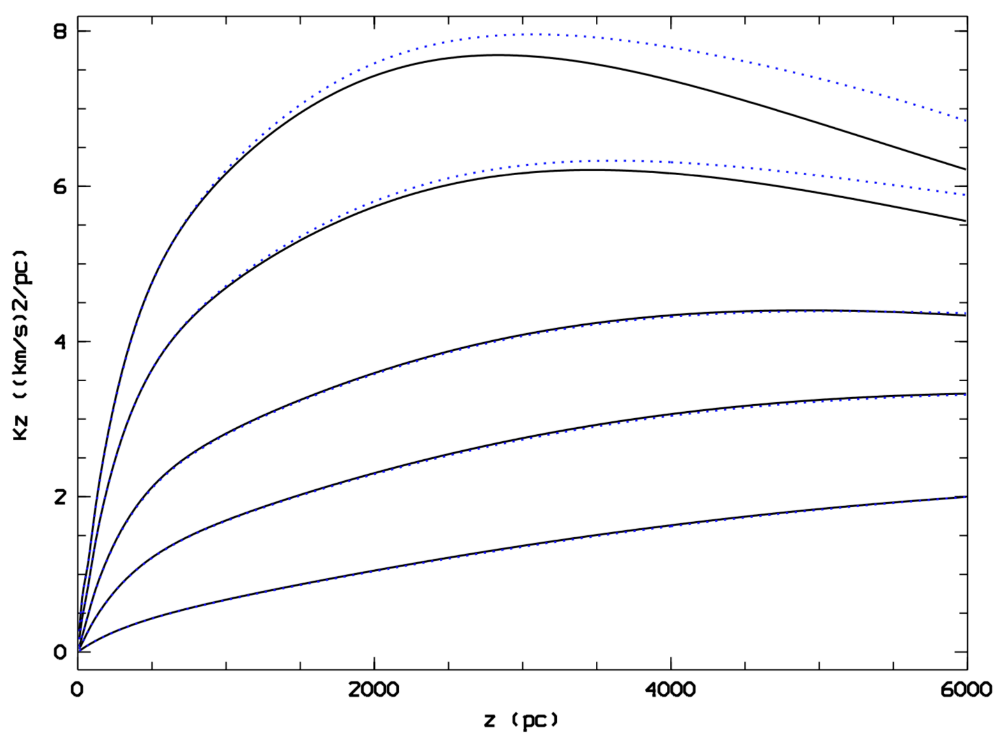

Fig. 7. Vertical force K_z versus z at R = (3.5, 4.5, 6.5, 8.5, 12.5 kpc) (*top to bottom*) from the BGM (black lines) and recovered K_z for a thick disc DF (blue dotted lines).

Bienaymé et al, 2015

Fit Gaia DR1 kinematics

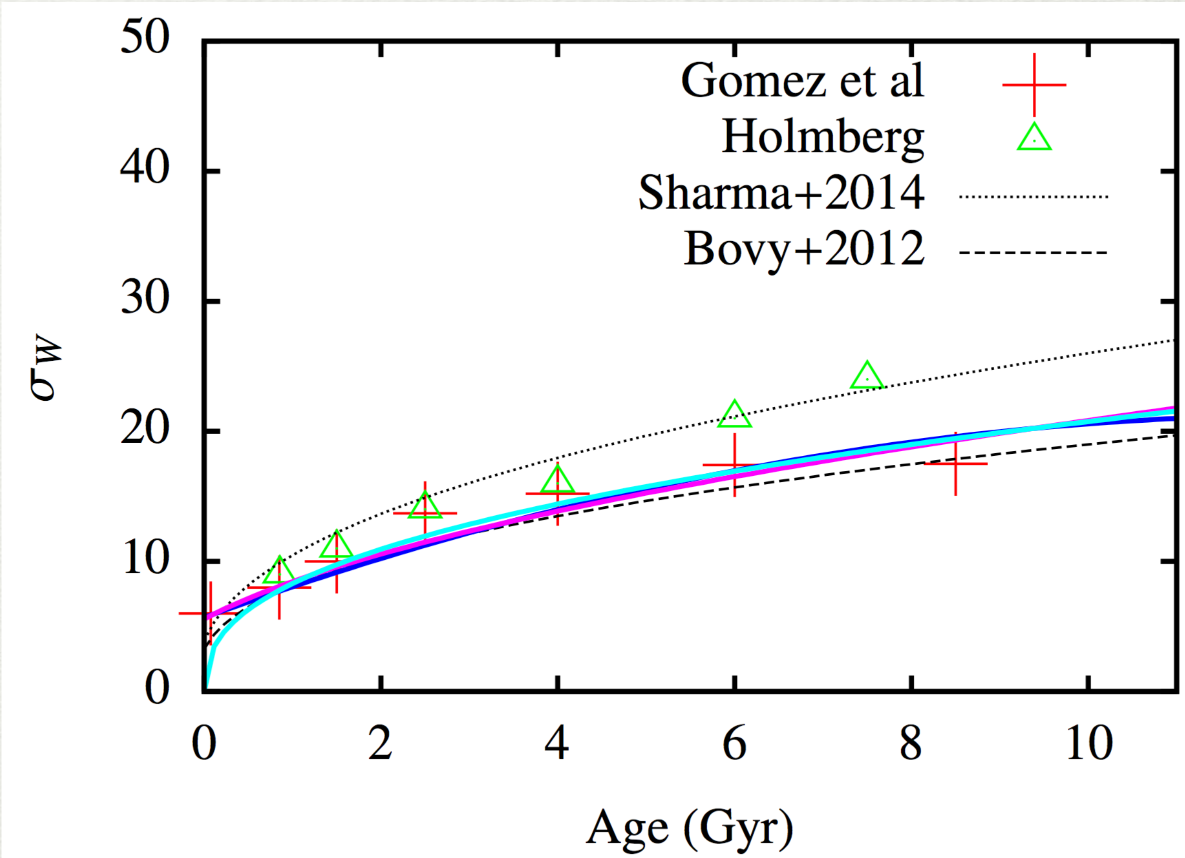

pmra

Solid: hot stars
Dashed: cool stars

Model
Gaia DR1

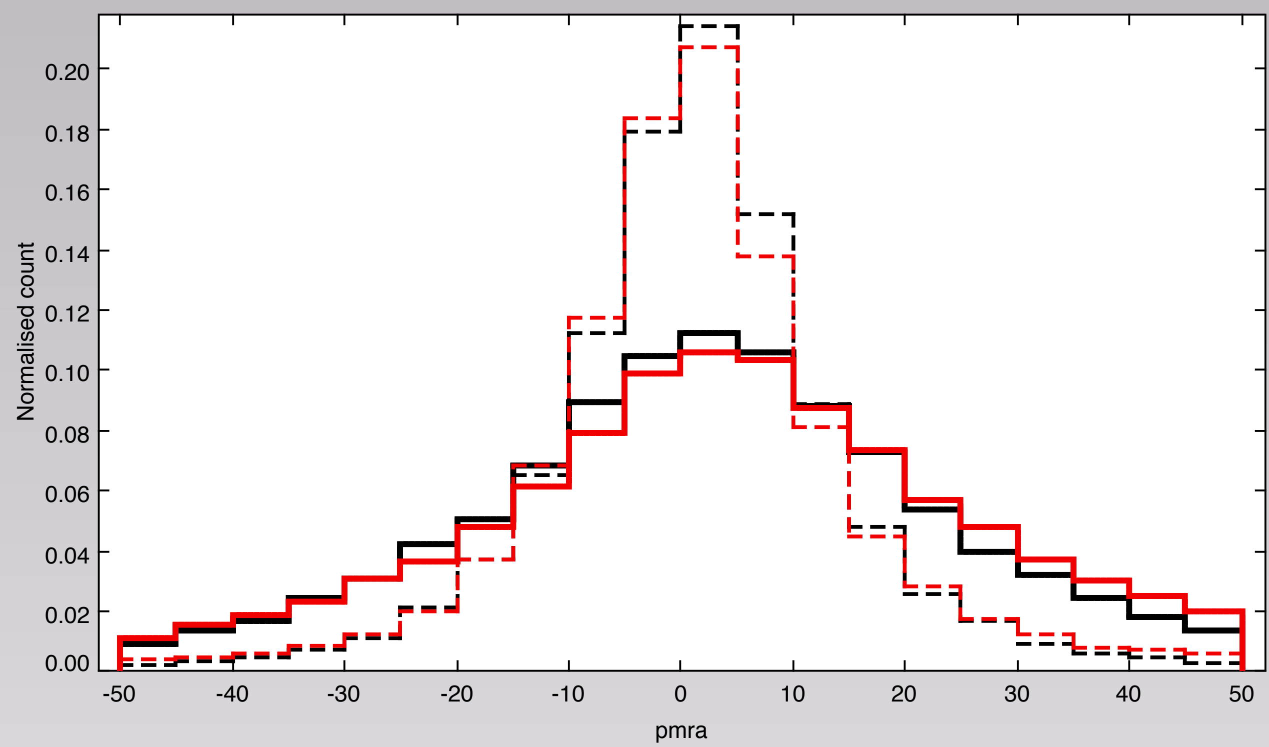

Radial Velocity

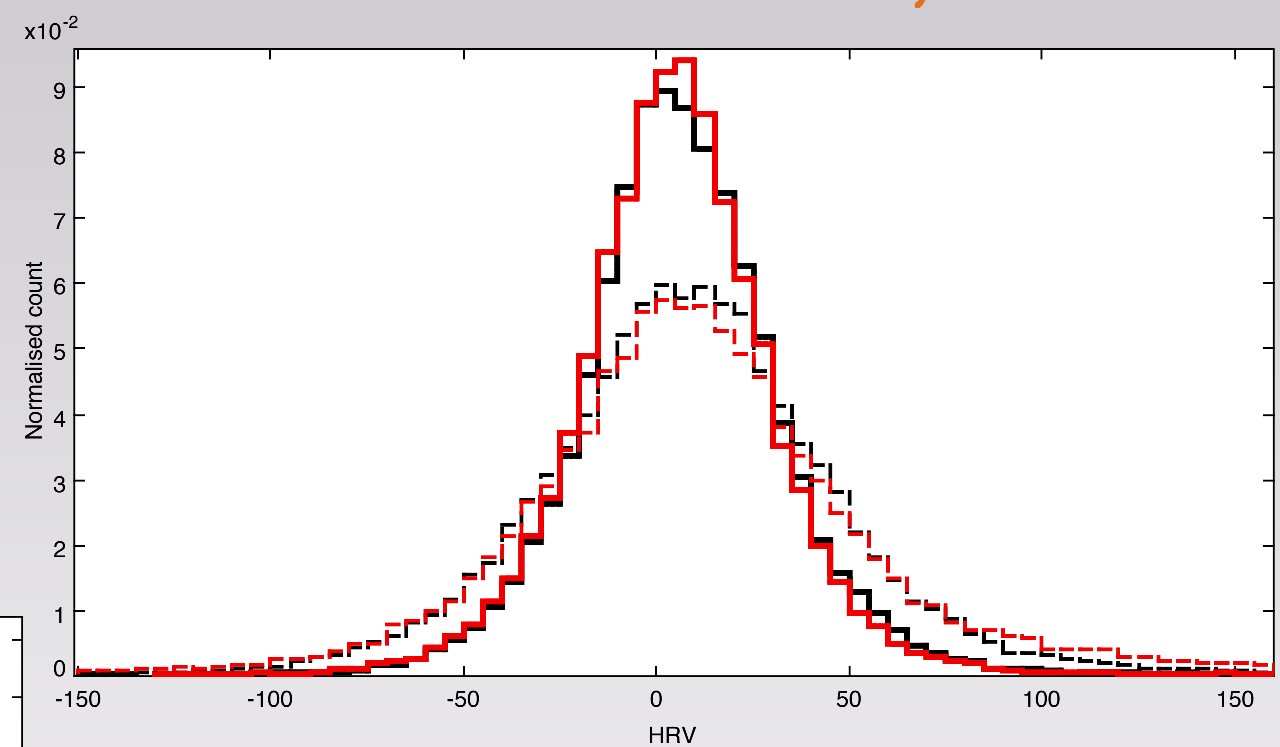

Gaia DR1

pmdec

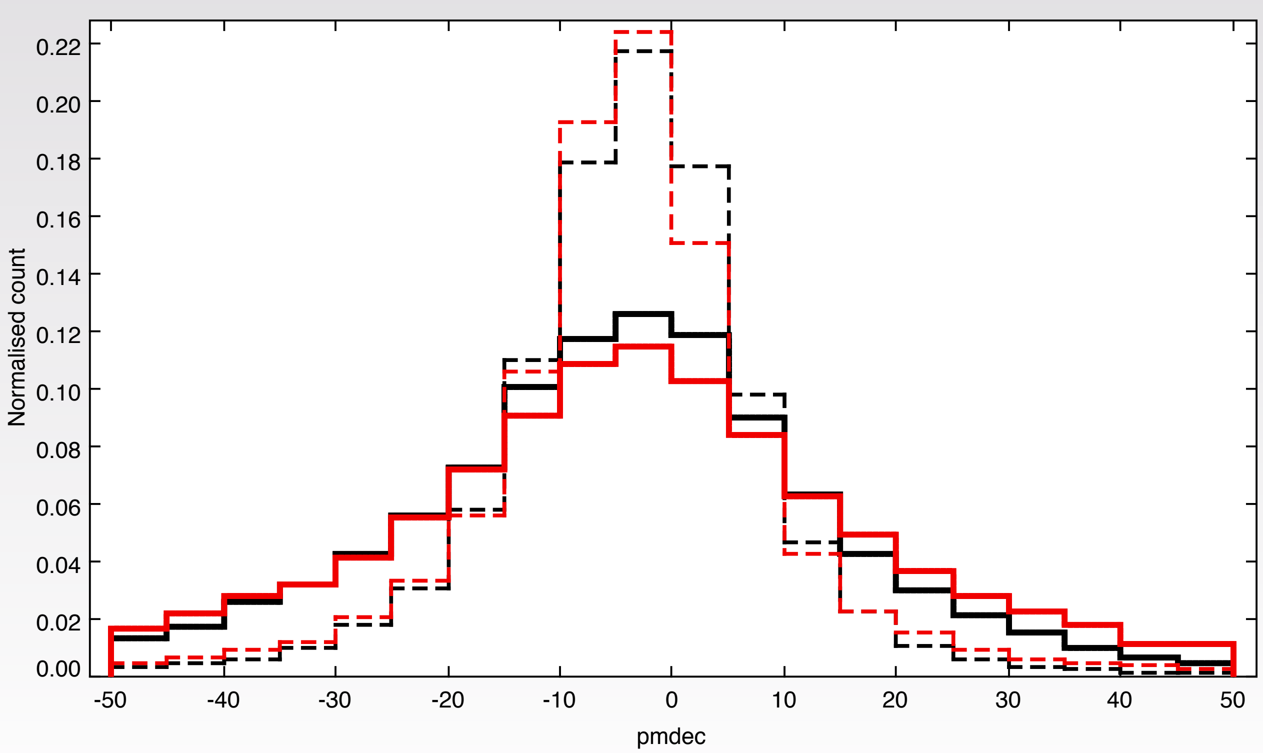

RAVE

Revised analysis with DR2 on-going

- Smooth model axisymmetric gives a reasonnable fit
- However, remaining systematics : non axisymmetry and non stationarity

Milky Way non-stationarity, non axisymmetry

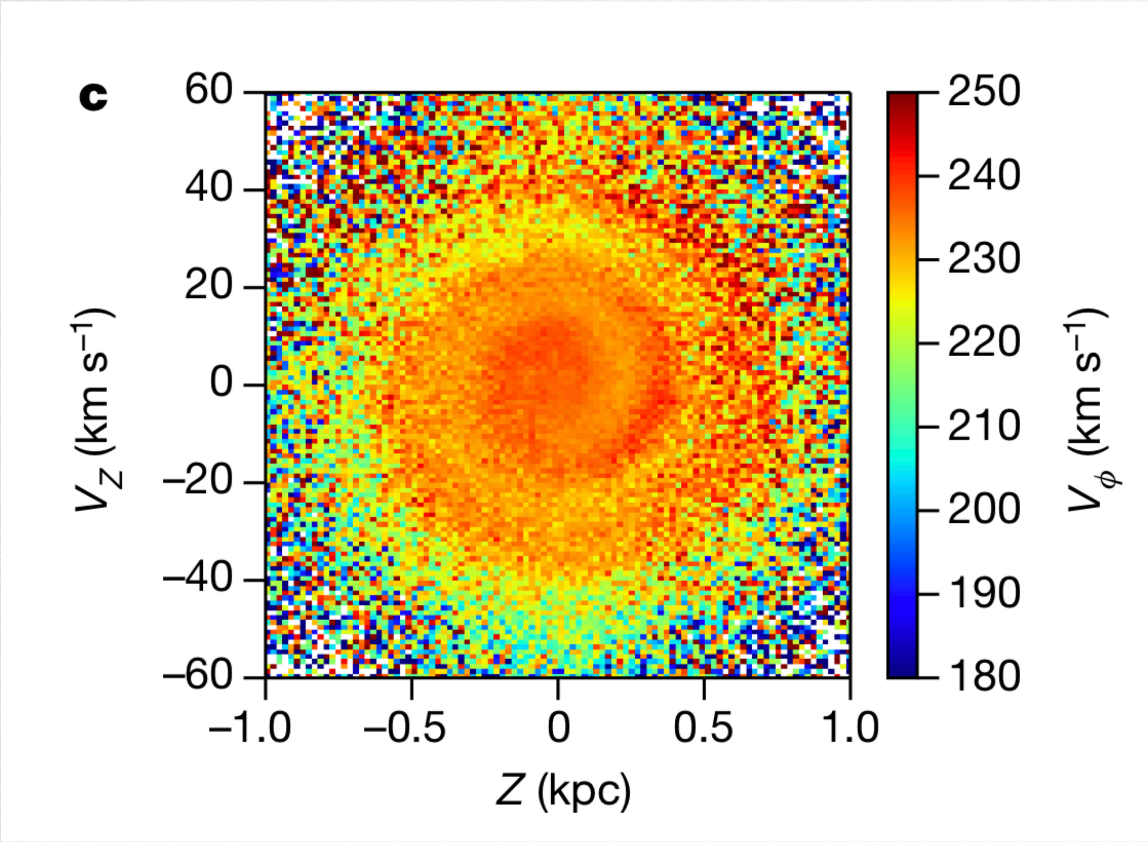

Antoja et al, 2018

Bennett & Bovy, 2018

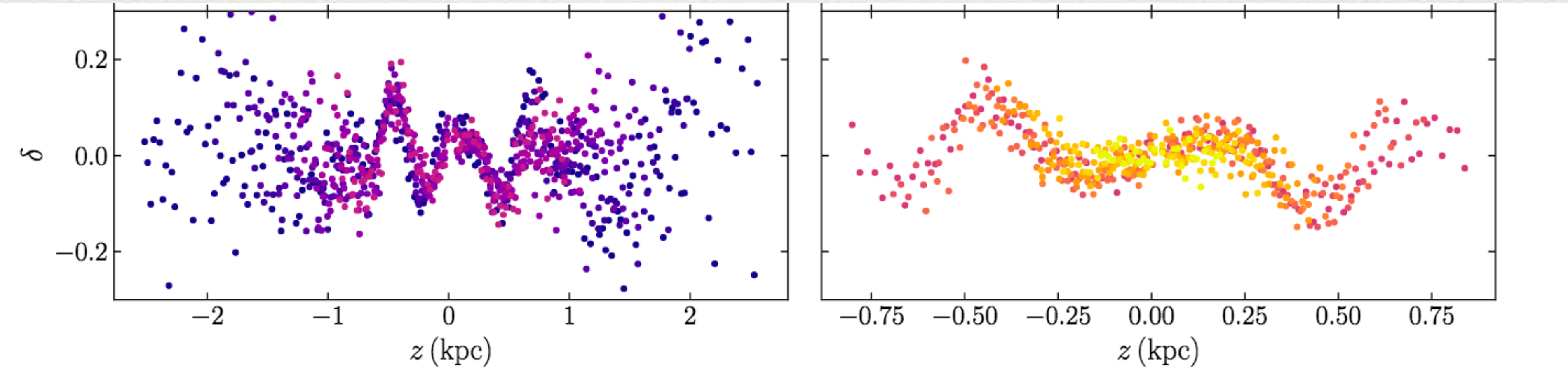

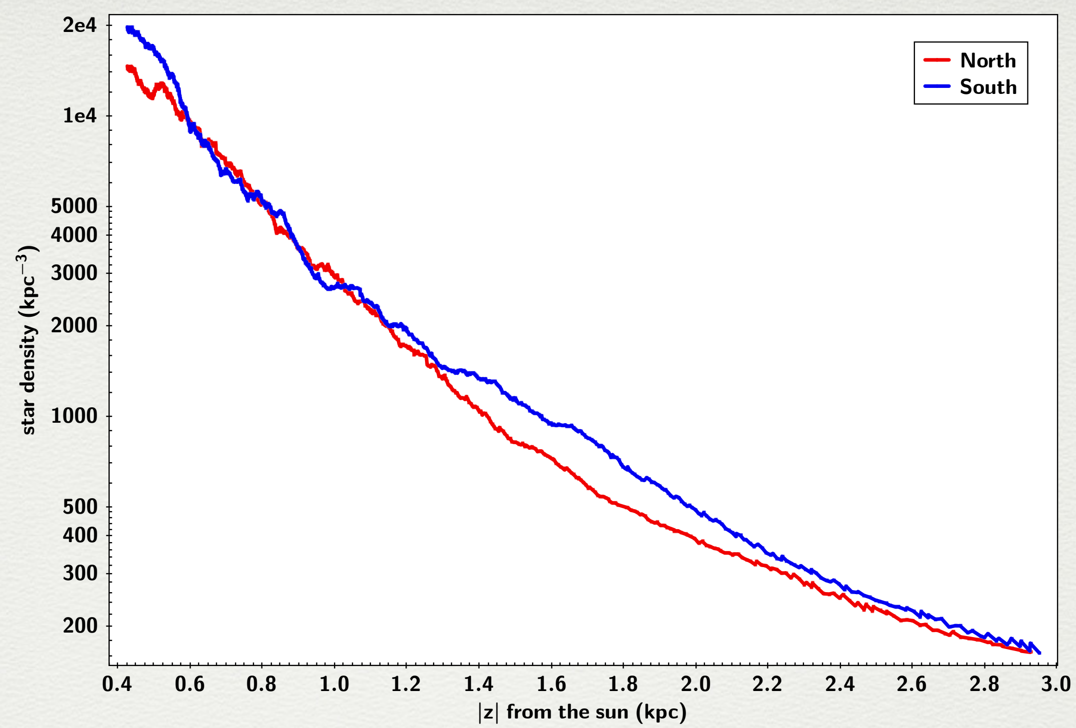

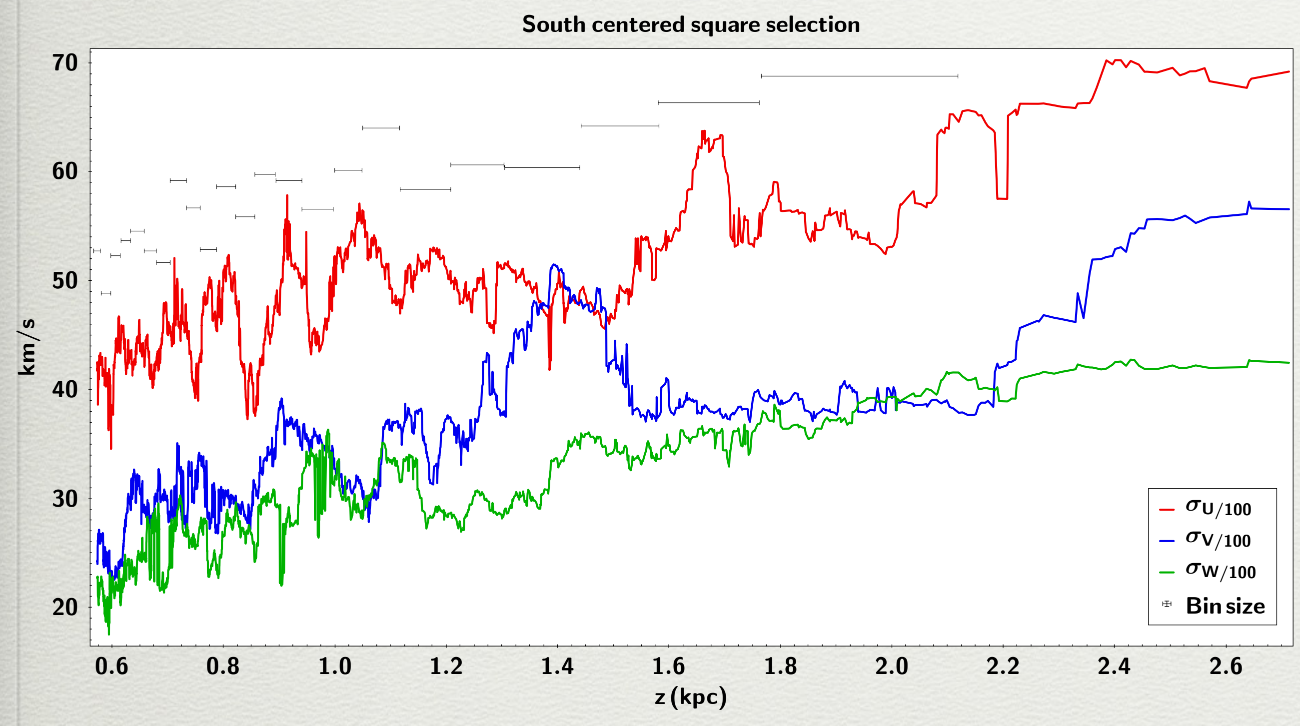

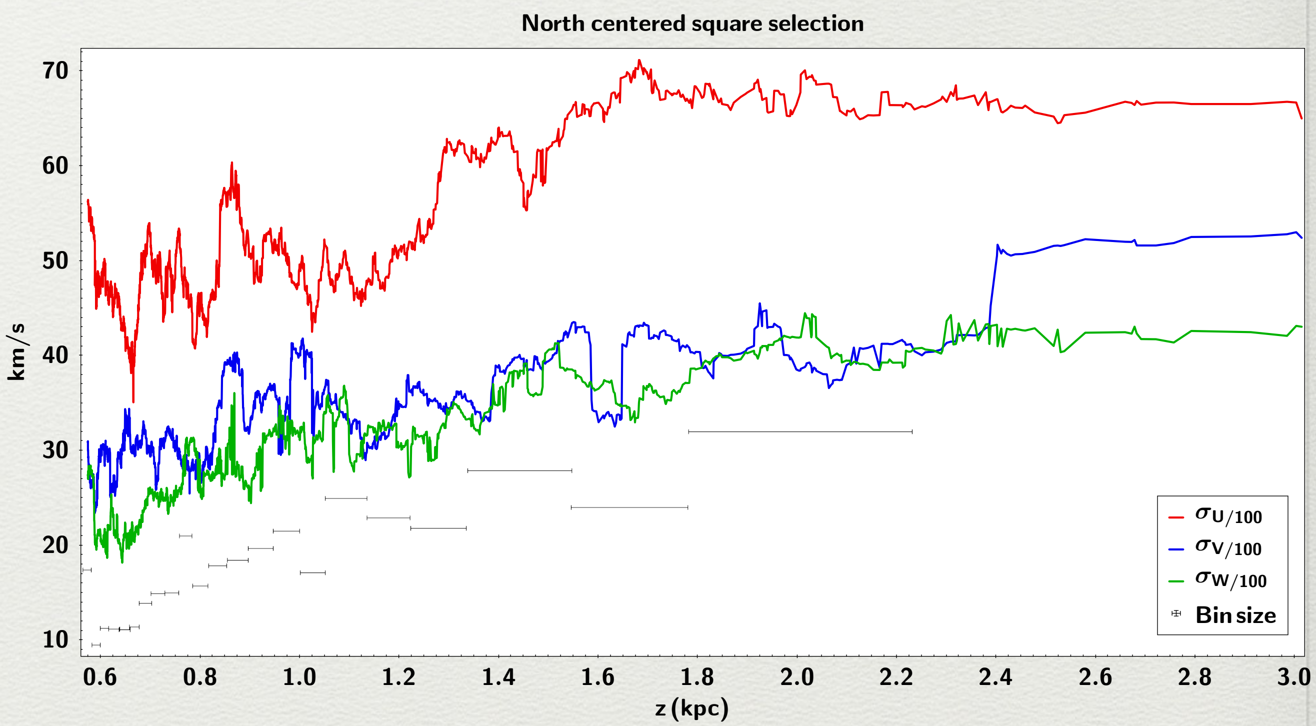

Salomon et al, 2019 in prep

Non axisymmetric model Gravpot

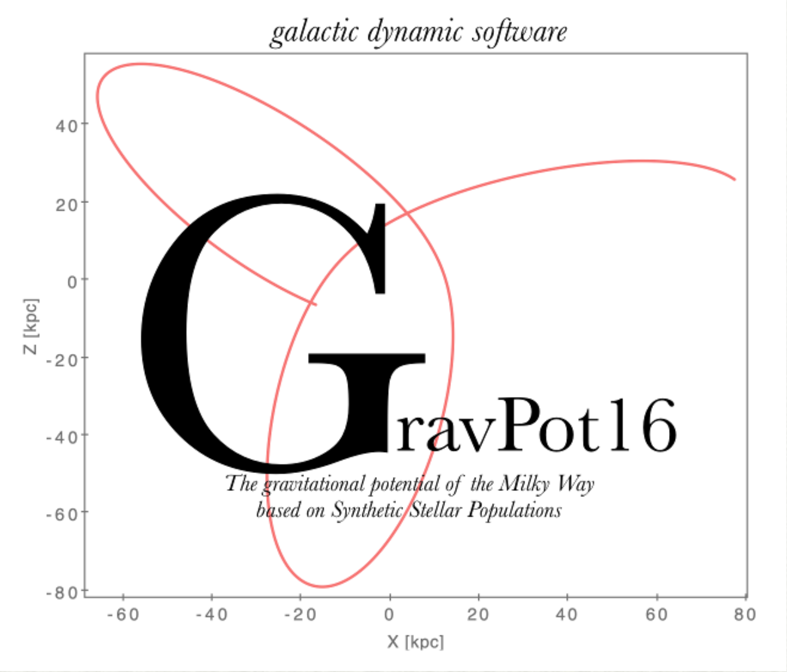

- Fernandez-Trincado, PhD 2017
- a new web service available. https:/ gravpot.utinam.cnrs.fr. (Fernandez-Trincado et al, 2019)

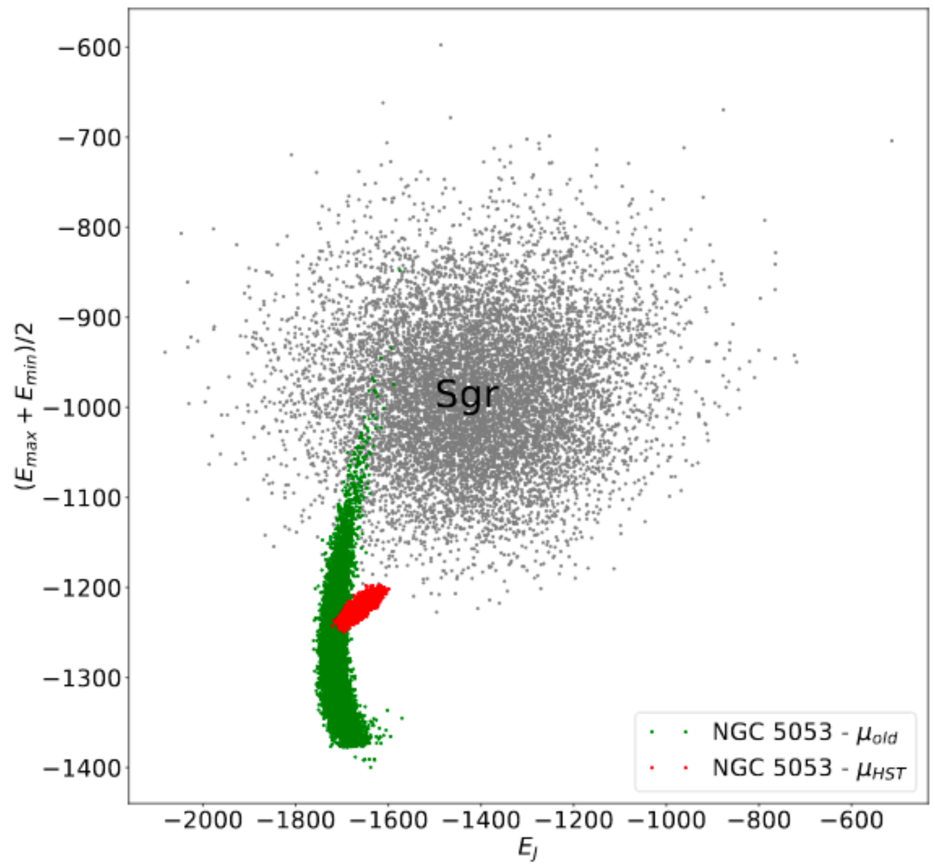

Figure 4. This diagram plots the "characteristic" orbital energy $(E_{min} + E_{max})/2$ versus the orbital Jacobi constant (E_J), in units of 1×10^5 km^2 s^{-2}, in the reference frame of the bar, and considering 1σ variations in a Gaussian Monte Carlo sampling (1×10^4 orbits). Grey dots are for the Sagittarius dwarf galaxy, green dots for NGC 5053 considering the absolute proper motion from Kharchenko et al. (2013), and red dots considering absolute proper motion from HST observations.

NGC5053 Orbital elements wrt Sag

Tang et al, 2018

2018ApJ...855...38T

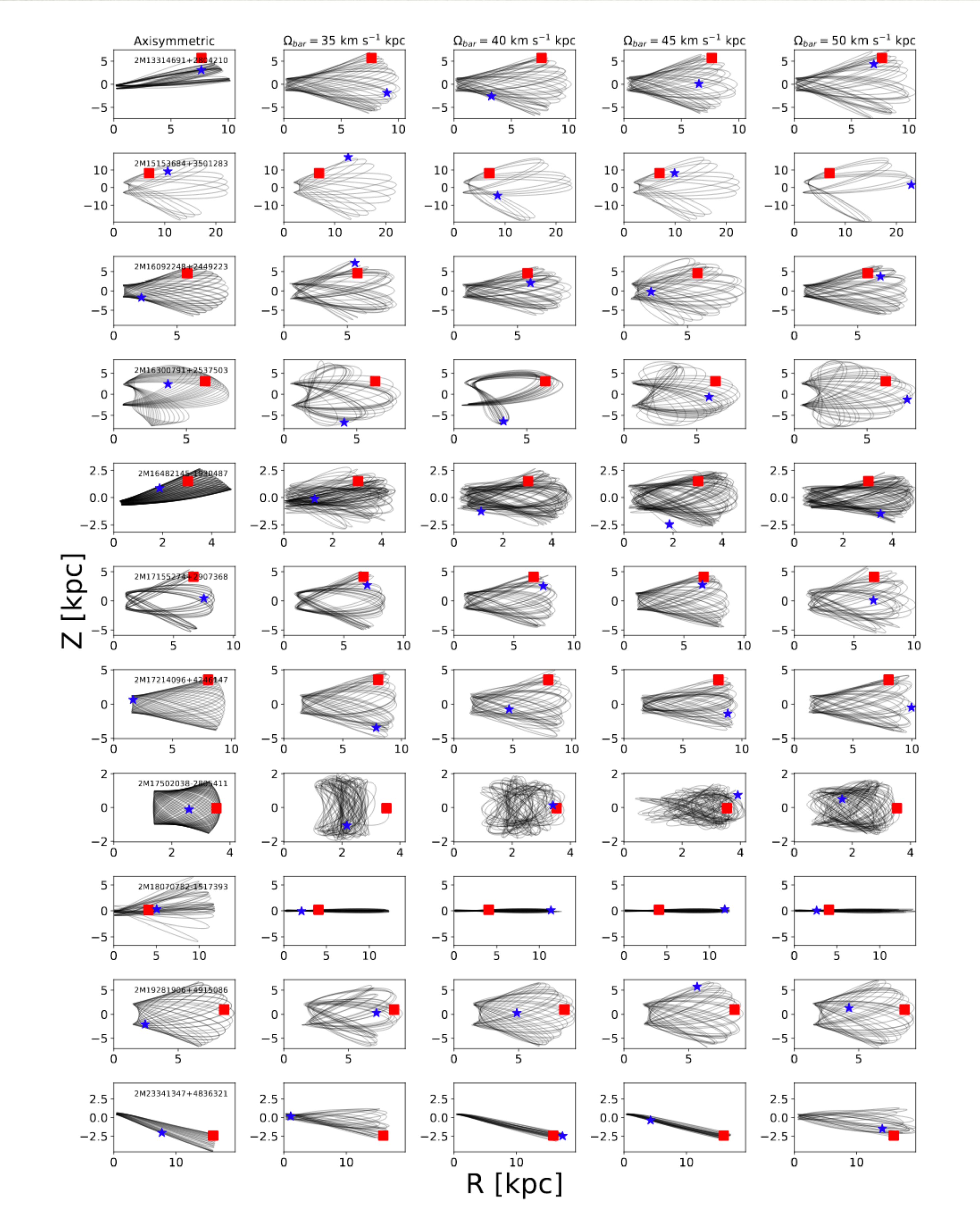

Fernandez-Trincado et al, 2019 arxiv/1904.05884

Look for globular cluster ejected stars in abundance space (SG stars)

Perspectives

- BGM-Fast: fit all populations on Gaia DR2 with G<18
- Combining spectroscopic data with Gaia to constrain the model, check the thick disc and bar scenarios of formation
- Spectro+asteroseismic analysis and clues for the disc formation
- Deep learning : improved classification based on detailed stellar evolutionary tracks, with abundances and asteroseismology (Lagarde et al, 2018)

Perspectives 2

- A new Gaia simulation (GUMS20 and GOG20) will be published in a few months implementing model fitting results from Gaia DR1 and DR2 ***(new IMF, SFH for thin disc, extinction map from DR2, kinematics from DR1).***

Hvala !